Integration of diagenesis, porosity evolution, and oil emplacement in lacustrine tight sandstone reservoirs: A review with illustrative cases from the major oil-bearing basins in China

Kelai Xi, Yingchang Cao, Rukai Zhu, Honggang Xin, Weidong Dan, and Helge Hellevang

ABSTRACT

Tight sandstone oil is currently one of the most important unconventional hydrocarbon resources in China. The coupling relationship between porosity evolution and oil emplacement determines the reservoir effectiveness and oil exploration potential in tight sandstones. Complex diagenetic alterations, however, make research on porosity evolution much more difficult than that on conventional sandstone reservoirs. This study examines the typical lacustrine tight sandstones from western to eastern China. The reservoir lithologies, characteristics, and paragenetic sequences of the diagenesis are reviewed, and an integrated analysis of diagenesis, porosity evolution, and oil emplacement is proposed.

Results demonstrate that diagenesis is influenced by rock composition and lithological associations. For example, calcite cementation is primarily controlled by the distance to the sandstone–mudstone interface, whereas zeolite cements are related to volcanic rock fragments. Furthermore, we established a porosity evolution recovery method with respect to the paleoburial depth (or time) of major diagenetic events, including the evaluation of the relationship between the thin section and helium porosity and oil emplacement. We clarified the formation time

Manuscript received May 5, 2022; provisional acceptance May 10, 2022; revised manuscript received June 25, 2022; revised manuscript provisional acceptance October 21, 2022; 2nd revised manuscript received November 11, 2022; 2nd revised manuscript provisional acceptance June 6, 2023; 3rd revised manuscript received July 18, 2023; 3rd revised manuscript provisional acceptance August 3, 2023; 4th revised manuscript received August 28, 2023; final acceptance October 5, 2023; preliminary ahead of print version published December 18, 2023.
DOI:10.1306/12212322063

AUTHORS

KELAI XI ~ *National Key Laboratory of Deep Oil and Gas, China University of Petroleum (East China), Qingdao, Shandong, China; xikelai@upc.edu.cn*

Kelai Xi is a professor at China University of Petroleum (East China). His research focuses on tight sandstone diagenesis, reservoir quality prediction, and unconventional oil and gas reservoir characterization. He is a corresponding author of this paper.

YINGCHANG CAO ~ *National Key Laboratory of Deep Oil and Gas, China University of Petroleum (East China), Qingdao, Shandong, China; cyc8391680@163.com*

Yingchang Cao is a professor at China University of Petroleum (East China). His research interests lie in the fields of sequence stratigraphy, sedimentology, and sandstone reservoir quality prediction. He is a corresponding author of this paper.

RUKAI ZHU ~ *Research Institute of Petroleum Exploration and Development, China National Petroleum Corporation, Beijing, China; zrk@petrochina.com.cn*

Rukai Zhu is a professor at Research Institute of Petroleum Exploration and Development, China National Petroleum Corporation. His research interests lie in the fields of sedimentology, reservoir quality prediction, and unconventional oil and gas reservoir characterization.

HONGGANG XIN ~ *Research Institute of Petroleum Exploration and Development, PetroChina Changqing Oilfield Company, Xi'an Shaanxi, China; xinhg_cq@petrochina.com.cn*

Honggang Xin is a senior engineer at Research Institute of Petroleum Exploration and Development, PetroChina Changqing Oilfield Company. His research interests lie in sandstone reservoir characterization and tight oil reservoir evaluation.

WEIDONG DAN ~ *Research Institute of Petroleum Exploration and Development, PetroChina Changqing Oilfield*

Company, Xi'an Shaanxi, China; dwd_cq@petrochina.com.cn

Weidong Dan is a senior engineer at Research Institute of Petroleum Exploration and Development, PetroChina Changqing Oilfield Company. His research interests lie in the fields of sedimentology and tight oil reservoir evaluation.

HELGE HELLEVANG ~ *Department of Geosciences, University of Oslo, Blindern Oslo, Norway; helge.hellevang@geo.uio.no*

Helge Hellevang is a professor at the University of Oslo. His research interests lie in the fields of reservoir diagenesis and low-temperature geochemistry.

ACKNOWLEDGMENTS

We are very grateful to the editors and anonymous reviewers for their careful work and thoughtful suggestions that helped to improve the manuscript. These research achievements were cofunded by the Innovation Research Group of the Natural Fund Committee (Grant No. 41821002), the Key Project of China National Petroleum Corporation (ZD2019-183-01-003), the Taishan Scholars Program (tsqn202306125), the National Natural Science Foundation of China (42072161), and the Fundamental Research Funds for the Central Universities (22CX07008A). We are also grateful to the Xinjiang, Changqing, and Jilin Oilfield Companies, PetroChina, for providing their in-house database and permission to publish.

and the underlying mechanisms. Three typical examples from the major oil-bearing basins in China were chosen to analyze the integration process of diagenesis, the porosity evolution of tight sandstones, as well as the coupling relationship between porosity evolution and oil emplacement. Tight sandstones characterized by different diagenetic alterations exhibit different coupling relationships between porosity evolution and oil emplacement. Our study can provide important guidance for reservoir quality prediction and oil exploration potential evaluation.

INTRODUCTION

Tight sandstone oil is one of the principal unconventional hydrocarbon resources increasing oil reserves and production in China and elsewhere (Jia et al., 2012; Zhao et al., 2012; Zou et al., 2013a, 2014). Exploration practices have demonstrated that tight sandstone oil and gas reservoirs are present in the majority of the petroliferous basins in China. Tight sandstone reservoirs are defined as having an average porosity lower than 10%, air permeability less than 1.0 md, or in situ permeability less than 0.1 md (Zou et al., 2012). They are characterized by continuous or quasi-continuous oil and gas accumulation (Schmoker, 2005), where reservoir quality is considered to be the most important controlling factor for the distribution of oil and gas (Camp, 2008; Zou et al., 2013b; Xi et al., 2015a). However, the diagenetic alteration has resulted in complicated porosity evolution processes and strong heterogeneities (Gluyas and Coleman, 1992; Gier et al., 2008; Lai et al., 2016; Rahman and Worden, 2016; Wang et al., 2017; Oluwadebi et al., 2018). The diagenesis of sandstones is controlled by several factors, such as rock composition, burial history, temperature, pressure, pore fluid properties, and tectonic evolution (Dutton and Loucks, 2010; Morad et al., 2010; Mahmic et al., 2018; Wang et al., 2018). Diagenesis in tight sandstones most likely formed at different burial stages as a result of rock composition and variable diagenetic environments in lacustrine basins (Bjørlykke, 2014; Zhang et al., 2015; Wei et al., 2016).

Diagenesis has been extensively studied in tight sandstone reservoirs. Previous research has focused mainly on cementation and dissolution mechanisms, including silica and carbonate cementation, authigenic clay mineral precipitation, and silicate or carbonate mineral dissolution (Gluyas et al., 2000; Lander and Bonnell, 2010; Metwally and Chesnokov, 2012; Anovitz et al., 2013; Hyodo et al., 2014; Xi et al., 2015a; Mu et al., 2016; Sample et al., 2017; Lai et al., 2018). The controls of diagenesis on reservoir quality have also been well documented for sandstone reservoirs (Stroker et al., 2013; Lai et al., 2016; Walker and Glover, 2018). Previous studies have identified several factors

influencing reservoir properties: (1) intergranular pores filled by lutaceous matrix, (2) reservoir pores in sandstones abundant with ductile detrital grains destroyed by strong compaction, (3) primary and secondary pores intensely cemented by carbonate or silicate minerals, and (4) the pore throat networks plugged by authigenic clay minerals (Worden and Burley, 2003; Zhang, 2008; Wang and Yue, 2012; Chen et al., 2015; Mahmic et al., 2018).

It is widely accepted that porosity during oil emplacement is key for the evaluation of oil exploration potential (Cao et al., 2018; Guo et al., 2018; Rosales et al., 2018). Thus, to improve the efficiency of oil exploration, the coupling relationship between porosity evolution and oil emplacement must be fully understood (Yang et al., 2016; Chen et al., 2017). This requires quantitative studies of the porosity evolution process during geologic time (Cao et al., 2018). Porosity evolution studies have been conducted for predrill prediction of tight sandstone reservoir quality in different basins, including quantitative statistics, and physical and numerical simulations (Mondol et al., 2007; Ajdukiewicz and Lander, 2010; Marcussen et al., 2010; Tobin et al., 2010). These models have provided porosity prediction methods for tight sandstone reservoirs controlled by different types of diagenesis, such as compaction, cementation, and dissolution (Taylor et al., 2010; Wang et al., 2013). In carbonate reservoirs, some quantitative diagenesis studies have also been used to predict the reservoir porosity and permeability (Al Khalifah et al., 2020; Mohammed Sajed et al., 2021; Rashid et al., 2022). Despite the substantial amount of work focusing on porosity evolution, the paleoburial depth (or geologic time) of the major diagenesis processes are still not well understood (Zhang et al., 2015; Wei et al., 2016; Ma et al., 2018; Busch et al., 2019). In previous studies, porosity loss by mechanical compaction was limited to the early stage of the diagenesis rather than considering the potential for compactional effects during later burial stages (Wei et al., 2016; Li et al., 2017; Lothe et al., 2018). These aforementioned studies have limited the understanding of the coupling relationship between tight reservoir formation and oil emplacement time. Therefore, integration of diagenesis, porosity evolution, and oil emplacement in tight sandstone reservoirs requires further research.

The Cretaceous Quantou Formation in the Songliao Basin, the Triassic Yanchang Formation in the Ordos Basin, and the Permian Jiamuhe Formation in the Junggar Basin are typical lacustrine basins with tight sandstone oil and gas fields in China. Many wells have been drilled in these basins, and most of the discovered oil fields have been developed. Core samples from other exploration wells and production well data are available for reservoir research. Due to the different geologic histories and rock composition, the diagenesis and porosity evolution processes vary significantly between these different tight sandstone reservoir areas. It is therefore valuable to fully integrate the integration processes of diagenesis, porosity evolution, and oil emplacement in different lacustrine tight sandstone reservoirs from across the various tight oil sandstone plays in China.

GEOLOGIC BACKGROUND

The Junggar Basin

The Junggar Basin is one of the most important oil-bearing basins in western China. The tectonic evolution of the basin can be summarized as four stages: (1) foreland oceanic basin, (2) foreland continental basin, (3) intracontinental sag, and (4) rejuvenated foreland basin (Kang et al., 2019). In ascending order, the stratigraphy of the Permian continental clastic deposits include the Jiamuhe, Fengcheng, Xiazijie, and Wuerhe Formations (Figure 1A). These formations are the major oil exploration and development targets. Oil exploration has shown that the Jiamuhe Formation is favorable for oil and gas accumulations, with hydrocarbon resources of approximately 14.8 BCM (10^9 m^3) (Yuan et al., 2017). The reservoirs, however, are tight (porosity <10% and permeability <1 md), which makes the oil and gas exploration more difficult than the Xiazijie and Wuerhe oil-bearing formations.

The Ordos Basin

The Ordos Basin is a polycyclic sedimentary craton basin located in the central part of China, covering an area of approximately 250×10^3 km^2. During the Middle to Late Triassic, fluvial-lacustrine sediments were deposited in the basin, forming the most important oil and gas reservoirs (Zhao et al., 2015). The formation that makes up the tight sandstone

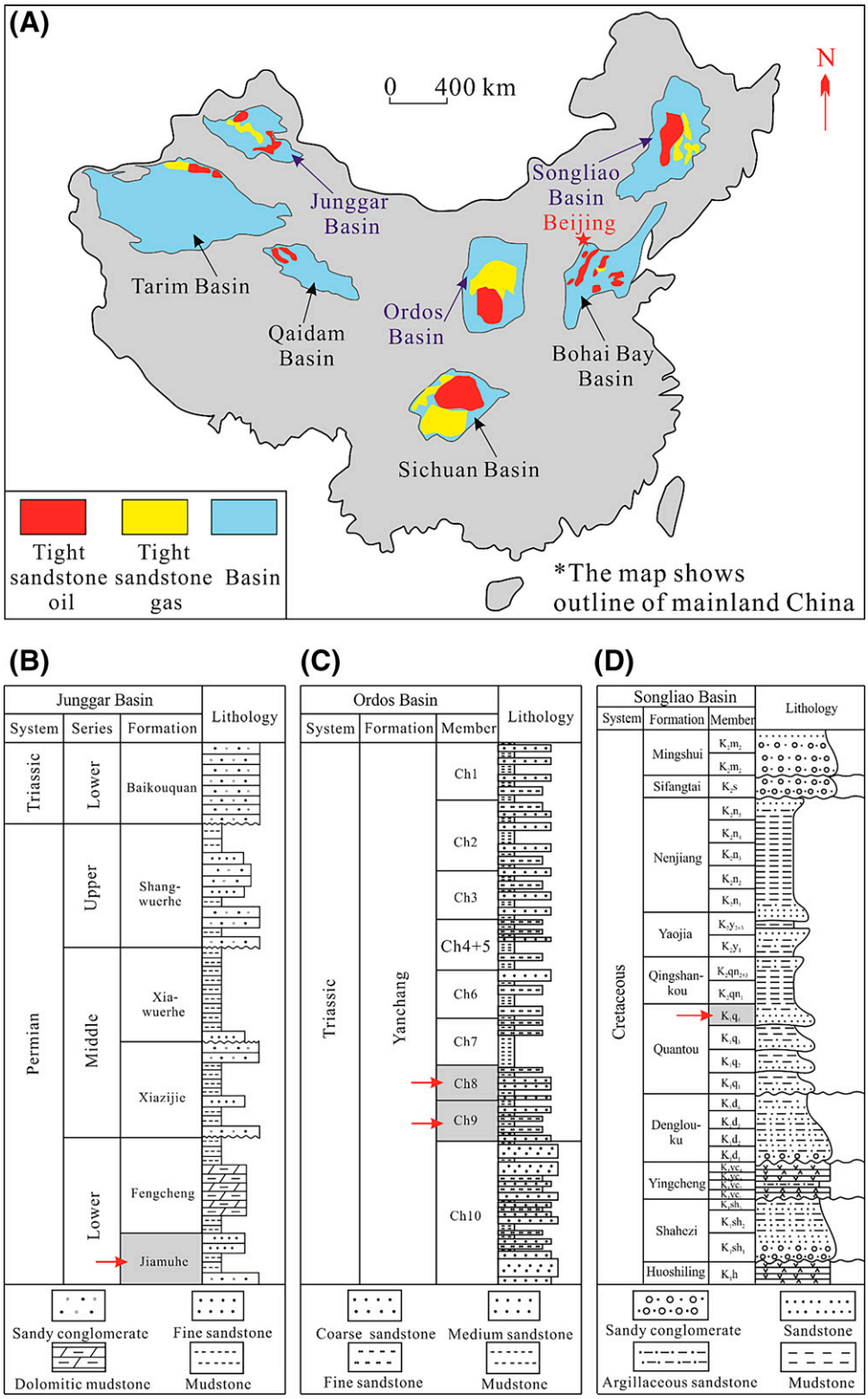

Figure 1. (A) Outline map of mainland China showing locations of the tight oil and gas basins in this study. (B) Stratigraphic profiles of the Permian in the Junggar Basin. (C) Stratigraphic profiles of the Triassic in the Ordos Basin. (D) Stratigraphic profiles of the Cretaceous in the Songliao Basin. The red arrows in (B–D) show the studied reservoir formations.

petroleum system is primarily the Upper Triassic Yanchang Formation (Duan et al., 2008). The Yanchang Formation ranges in thickness from approximately 200 m (656.17 ft) to 1400 m (4593.18 ft) throughout the basin, which is further divided into 10 members (Figure 1B), namely Chang 1–Chang 10 from top to bottom of the formation (Duan et al., 2008). Among them, Chang 4, 5, and 7 members deposited thick shales, being excellent source rocks. Other members mainly consist of sandstones with some interbedded mudstones. The Chang 8 and 9 members are mainly tight sandstones (Figure 1B). The Yanchang Formation is one of the most typical areas for tight sandstone oil exploration and development in China (Zhou et al., 2016).

The Songliao Basin

The Songliao Basin is a Jurassic–Neogene lacustrine basin in northeastern China. The basin underwent four tectonic evolution stages: a prerift phase, a synrift phase, a postrift phase, and a compression phase (Zhang et al., 2009). The sedimentary section comprises Cretaceous, Paleogene, Neogene, and Quaternary (Xi et al., 2015a). The formations involving petroleum systems are mainly the Lower and Upper Cretaceous, which can be further divided into several source rock and reservoir combinations (Figure 1C). The Lower Cretaceous Quantou Formation was deposited during the depression period of the tectonic evolution, and consists mainly of deltaic sandstones. The basin has experienced high geothermal gradients throughout most of its history, resulting in complicated diagenetic alterations of the sandstone reservoirs. Presently, the reservoir is tight and heterogeneous, significantly controlling the hydrocarbon distribution in this area (Li et al., 2013).

METHODS

Rock composition data as well as reservoir porosity and permeability data were obtained from the Research Institute of Petroleum Exploration and Development of the Jilin, Changqing, and Xinjiang Oilfield Companies, PetroChina. In addition, permission was granted to use some reservoir porosity and permeability data obtained from previously published reports. Core samples were also obtained from the Changqing, Xinjiang, and Jilin Oilfield Companies. Specifically, 216 core samples from 21 wells from the Permian Jiamuhe Formation were obtained from the Junggar Basin (Xinjiang Oilfield Company), more than 500 core samples and 2713 reservoir porosity and permeability data from 32 wells from the Triassic Yanchang Formation were obtained from Ordos Basin (Changqing Oilfield Company), and 743 core samples and more than 8000 reservoir porosity and permeability data from 40 wells from the Cretaceous Quantou Formation were collected from the Songliao Basin (Jilin Oilfield Company).

Using these core samples and data, reservoir diagenesis, pore characteristics, oil occurrence, and porosity evolutions were investigated. Standard petrographic thin sections were prepared from the core samples to analyze the rock composition and diagenetic features. A scanning electron microscope (SEM) was also used to describe the various pore types. Several samples with newly crushed surfaces were coated with carbon and observed under a Quanta 450 FEG cold field emission SEM at an accelerating voltage of 20 keV. The sample chamber was high vacuum and the working distance was set at 10 mm. According to the pore types and their sizes, the magnification ranges from approximately 1000 to 5000 times. Fluid inclusion data and cathode luminescence (CL) were also used to establish the diagenetic sequences. Digital image analysis of the photomicrographs was used to quantify the porosity observed in thin sections. Fluorescence observation of thin sections was used to determine the presence of oil in the tight sandstones.

Blue or red epoxy resin-impregnated thin sections were prepared for the analysis of reservoir pore spaces, diagenesis, and rock compositions. The thin sections were partly stained with Alizarin Red S and K-ferricyanide for the identification of carbonate minerals (Proia and Brinn, 1985). The content of primary and secondary pores, quartz cement, carbonate cements, and laumontite cement were calculated through micrograph image analysis. After scanning the whole thin section under the microscope, a field of view (FOV) was selected to represent the studied samples, according to the rock composition and rock structure. In this FOV, the cement and pores were identified under the Zeiss Axioscope A1 APOL digital transmission microscope and sketched on computer using CorelDRAW software (version 20.0.633).

The total area of each cement type and pore was captured by the microscopes and measured using Image-Pro Plus software, and the percentages of the diagenetic events were then calculated. To obtain accurate content, at least 20 micrographs for each sample were analyzed, and the average values were regarded as the content of each kind of cement and pore. Authigenic and some detrital clay minerals were observed under a Quanta FEG 450 SEM equipped with an energy-dispersive x-ray spectrometer. For the samples containing carbonate cements, CL analyses were performed using an Olympus microscope equipped with a CL8200-MKS CL instrument. Homogenization temperature of fluid inclusions were measured using a calibrated Linkam THMSG 600 heating and cooling stage. All of these analyses were conducted in the Key Laboratory of Deep Oil and Gas, China University of Petroleum.

RESULTS

Reservoir Lithologies

Detrital components are the most important factor controlling mechanical compaction and chemical diagenesis in tight sandstones (Rosales et al., 2018; Wang et al., 2018). The petrographic results show that the composition of the framework grains (quartz, feldspar, and rock fragments) varies from one basin to another (Figure 2). In the Permian Jiamuhe tight sandstone reservoirs of the Junggar Basin, the rocks are classified as litharenite (Figure 2A; Table 1); the Triassic Yanchang Formation sandstone reservoirs of the Ordos Basin are predominantly lithic arkose, with small amounts of arkose and feldspathic litharenite (Figure 2B; Table 1); and feldspathic litharenite and lithic arkose are the main components of the Cretaceous Quantou Formation sandstone reservoirs of the southern Songliao Basin (Figure 2C; Table 1).

Reservoir Pore Types

Pores of the tight sandstone reservoirs also varied across the lacustrine oil-bearing basins. Pores in the Permian Jiamuhe Formation of the Junggar Basin are generally associated with laumontite dissolution pores (Figure 3A, B). For these sandstone reservoirs, the laumontite dissolved strongly, forming large amounts of intergranular pores, increasing the pore throat connectivity, and significantly improving the reservoir properties (Figure 3A). Primary pores and feldspar dissolution pores are two major types of reservoir volumes found in the Triassic Yanchang Formation in the Ordos Basin and the Cretaceous Quantou Formation in the Songliao Basin (Figure 3C–F). For the Triassic Yanchang Formation of the Ordos Basin, the primary intergranular pores are modified by partial chlorite coatings (Figure 3C, D), and the intragranular pores are generally the result of feldspar dissolution (Figure 3C, D). Thus, the pore throat radii for these reservoirs are small and connectivity is relatively poor (Figure 3C, D), resulting in an extremely low permeability (<1.0 md). In tight sandstones of the Cretaceous Quantou Formation in the Songliao Basin, primary pores are distributed mainly

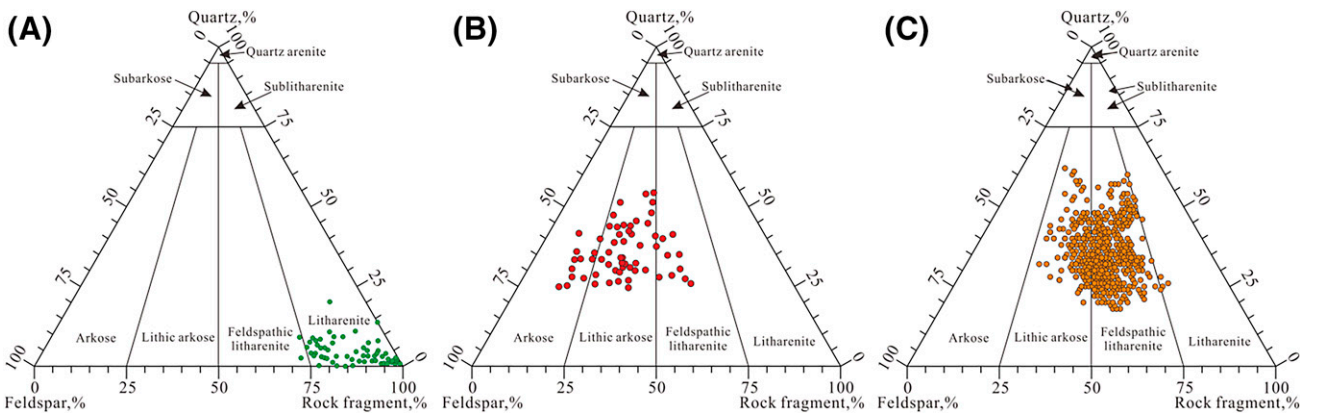

Figure 2. Rock composition characteristics of tight sandstones for the studied samples using the Folk (1974) classification. (A) Permian Jiamuhe Formation tight sandstone reservoirs in the Junggar Basin. (B) Triassic Yanchang Formation tight sandstone reservoirs in the Ordos Basin. (C) Cretaceous Quantou Formation tight sandstone reservoirs in the Songliao Basin (modified from Xi et al., 2015a).

Table 1. The Rock Composition of Tight Sandstones in Three Typical Basins of China

Basin	Formation	Quartz, %			Feldspar, %			Rock Fragment, %		
		Min	Max	Avg	Min	Max	Avg	Min	Max	Avg
Junggar Basin	Permian Jiamuhe	0.1	9.1	2.1	0.1	32.0	19.7	67.0	99.2	79.2
Ordos Basin	Triassic Yanchang	25.0	58.0	41.3	22.0	54.0	33.7	4.2	33.0	26.0
Songliao Basin	Cretaceous Quantou	32.1	62.4	42.9	10.3	42.8	26.0	12.7	47.6	31.1

Abbreviations: Avg = average; Max = maximum; Min = minimum.

in the areas of rigid grains (i.e., quartz and feldspars) (Figure 3E, F). Furthermore, feldspar dissolution in the Cretaceous Quantou Formation of the Songliao Basin commonly occurs from the edge to the center of the grains, enlarging the intergranular pores and improving pore throat connectivity (Figure 3E–I).

Reservoir Diagenesis

Tight sandstones in the lacustrine oil-bearing basins of China have experienced many stages of diagenetic modification, resulting in complicated porosity and permeability evolution processes. Compaction,

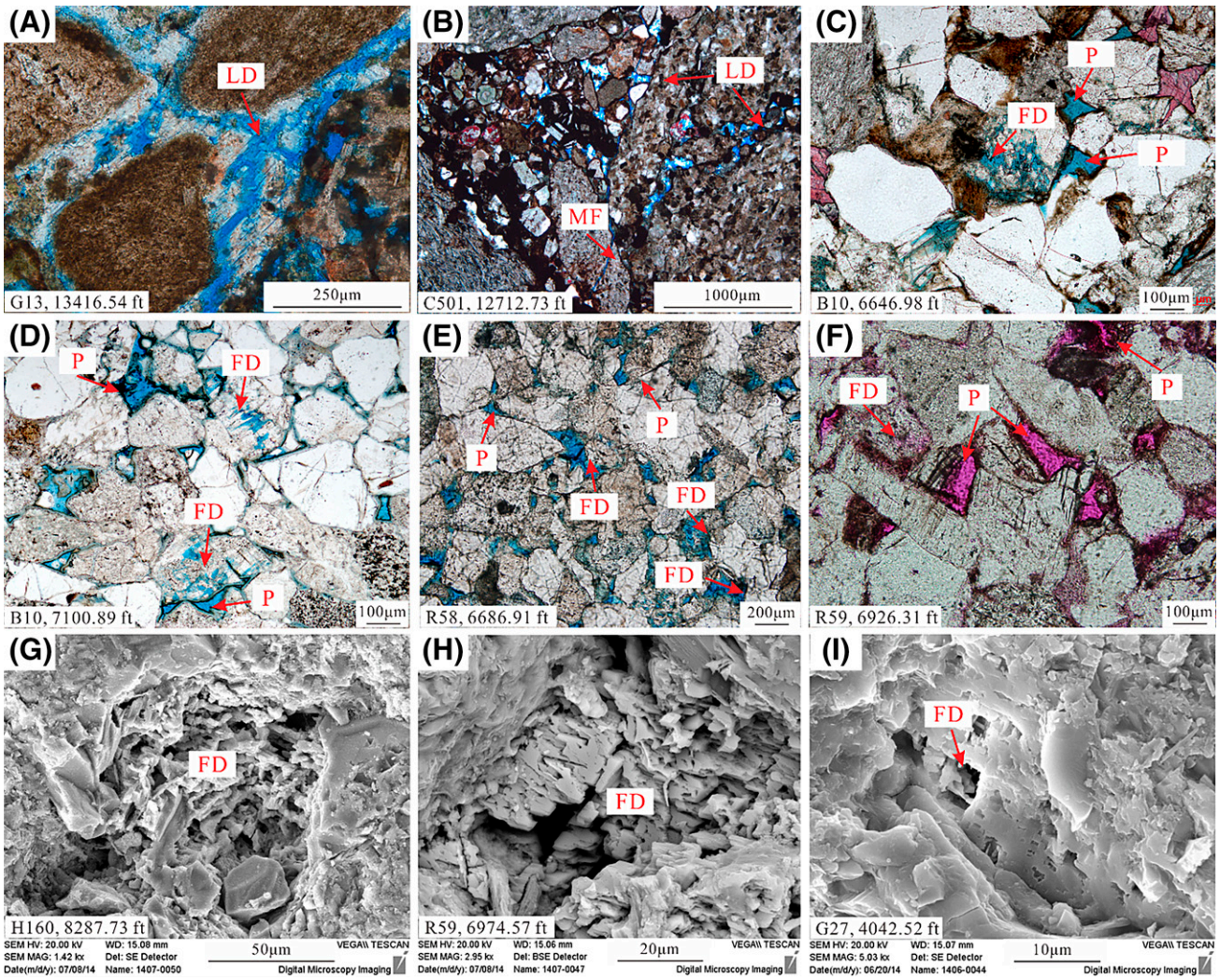

Figure 3. Pore types in lacustrine tight sandstone reservoirs. Sample number and depth labeled at lower left. (A, B) Laumontite dissolution (LD) pores in tight sandstone reservoir of the Junggar Basin. (C, D) Feldspar dissolution (FD) pores and primary (P) pores in tight sandstones of the Ordos Basin. (E, F) FD pores and P pores in tight sandstones of the Songliao Basin. (G–I) FD pores under scanning electron microscope (SEM). HV = high voltage; KV = kilovolt; MAG = magnification; MF = microfracture; SE = secondary electron; WD = working distance.

cementation, and dissolution are the key diagenetic events influencing reservoir qualities. Mechanical compaction is the principal cause of the porosity and permeability destruction. Cementation is an additional volumetrically predominant diagenesis, which includes precipitation of several types of authigenic minerals. Among these are carbonate cements, siliceous cement, zeolite cements, and authigenic clays dominate. In addition, minor cements, including pyrite, albite, and anhydrite, were observed. Both detrital grains and intergranular cements have been dissolved during the burial processes. Except for a relatively strong compaction in most of the tight sandstone reservoirs, the authigenic minerals and dissolution characteristics exhibited significant differences across the study areas.

Compaction

Compaction was observed to play the most important role in the reservoir porosity loss processes. Detrital grains in lacustrine tight sandstone reservoirs exhibit concavo-convex grain contacts. Deformed ductile grains also show evidence of extreme compaction, whereas a number of brittle grains are fractured. Intergranular volume (IGV) is a measure of pore plus cement volume that is able to effectively reflect the degree of mechanical compaction (Bjørlykke, 2014). The IGV in the investigated lacustrine tight sandstones generally lies within the range of 12% to 21%, indicating relatively strong mechanical compaction. Mechanical compaction accounts for approximately 50% to 65% of the total porosity loss during the burial processes. The lower IGV values are largely related to the abundance of ductile volcanic grains. In general, the IGV of the lacustrine tight sandstones have been shown to increase with increasing quartz grain content (Xi et al., 2015a, 2019a).

Carbonate Cementation

Carbonate cements are widely distributed in the studied lacustrine oil-bearing basins, with calcite, ferroan calcite, and ankerite observed as the major types (Figure 4A–D). There are in addition smaller amounts of dolomite, siderite, and dawsonite. Calcite, ferroan calcite, and ankerite are present in the Quantou Formation in the Songliao Basin (Figure 4A, C, D). Calcite was the dominant carbonate cement observed in the Triassic Yanchang Formation of the Ordos Basin (Figure 4B). Carbonate cementation, however, is absent through most of the Permian Jiamuhe Formation tight sandstone reservoir intervals in the Junggar Basin. The distribution of carbonate cements in the sandstones is often closely associated in proximity to interbedded mudstones, which are thought to have provided the source of calcium and carbon for carbonate precipitation (Xi et al., 2015a; Zhou et al., 2016; Lai et al., 2017). This agrees with our results, in which, in general, carbonate cements were observed at a greater intensity along the interface of sandstones with adjacent mudstones (Figure 5A). Tight sandstone reservoirs within a radius of 1.0 m (3.28 ft) to sandstone–mudstone interfaces were extensively cemented by calcite, whereas the carbonate cement content rapidly decreased at distances greater than 1.0 m (3.28 ft) away from the mudstone contact (Figure 5A). As a result, the interbedded layers of thin sandstones are always very tight, whereas high-quality reservoirs are distributed mainly in the central part of thick sandstone layers.

Siliceous Cementation

Quartz overgrowth is the predominant siliceous cement found in the studied lacustrine tight sandstones. Although the presence of siliceous cements is extensive in the tight sandstone reservoirs of China, their contents vary in different study areas. Only less than 0.5% of quartz overgrowth was observed in the Permian Jiamuhe Formation of the Junggar Basin. In the Triassic Yanchang Formation of the Ordos Basin, quartz overgrowths are small in size, and thus have minimum impact on reservoir quality. In contrast, the quartz overgrowths of the Cretaceous Quantou Formation in the Songliao Basin are larger in size, with a width of 30 to 100 μm (9.84×10^{-5} ft–3.2×10^{-4} ft) (Figure 4D–F), and are the volumetrically predominant cementing agent. The authigenic quartz partly or completely fills the intergranular pore spaces of the Cretaceous Quantou Formation in the Songliao Basin (Figure 4D–F). The IGV increases with decreasing cement content when cement constituted less than approximately 4% (Figure 5B). This can be attributed to the presence of quartz cements as overgrowth (Figure 4D, E), strengthening the mechanical resistance of the sandstones and protecting the intergranular pores. However, for quartz

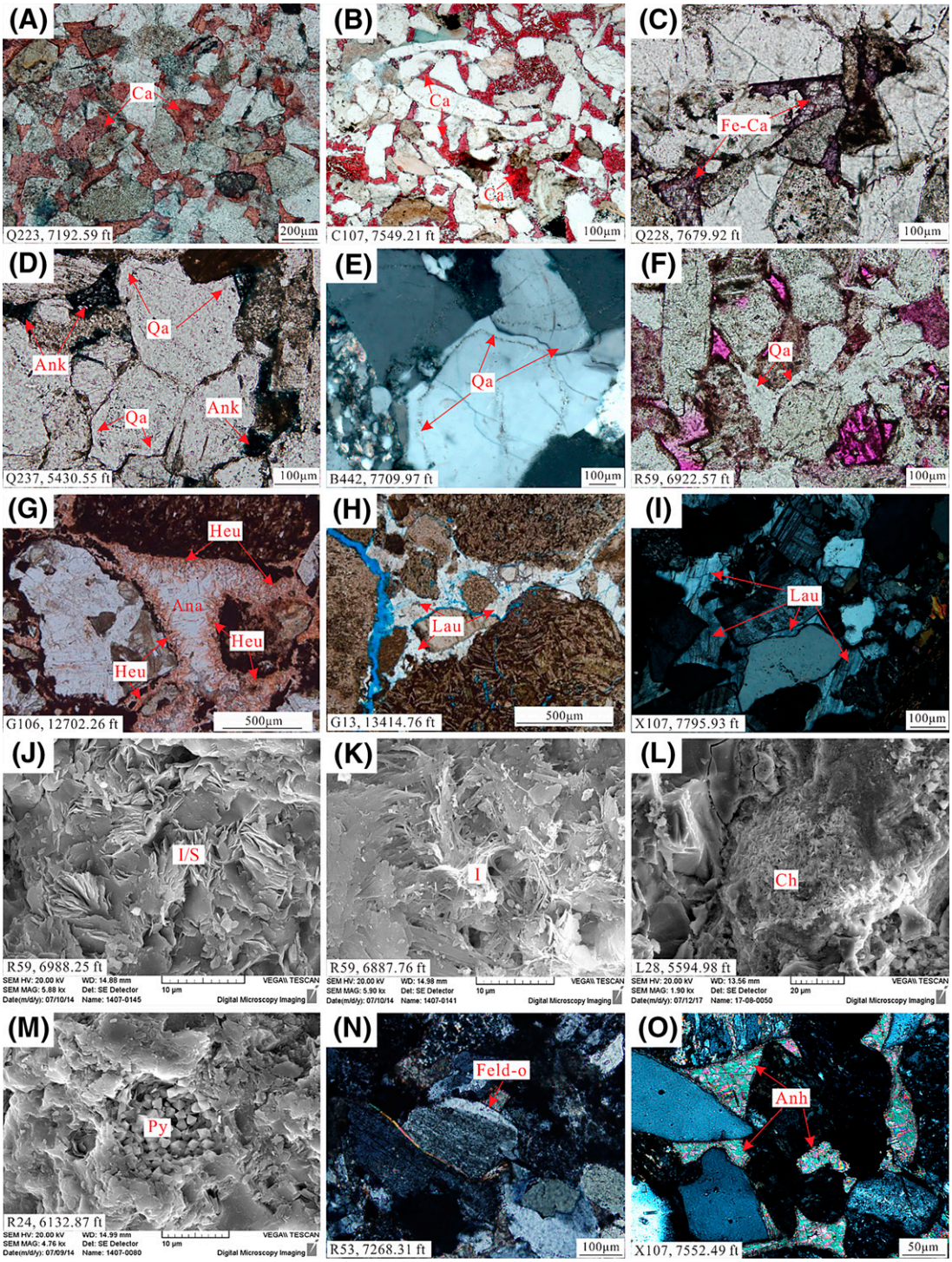

Figure 4. Characteristics of authigenic mineral cementation in lacustrine tight sandstone reservoirs. Sample number and depth labeled at lower left. (A, B) Calcite (Ca) cementation in lacustrine tight sandstone reservoirs. (C) Ferro-calcite (Fe-Ca) cementation in lacustrine tight sandstone reservoirs. (D) Ankerite (Ank) cementation in lacustrine tight sandstone reservoirs. (E) Quartz (Qa) overgrowth in lacustrine tight sandstone reservoirs. (F) Authigenic Qa cementation in lacustrine tight sandstone reservoirs. (G) Analcite (Ana) was replaced by heulandite (Heu) in tight sandstone reservoirs. (H, I) Laumontite (Lua) cementation in lacustrine tight sandstone. (J) Mixed-layer illite/smectite (I/S) in tight sandstone reservoirs of Songliao Basin. (K) Illite (I) in tight sandstone reservoirs of the Songliao Basin. (L) Chlorite (Ch) coating in tight sandstone reservoirs of the Ordos Basin. (M) Authigenic pyrite (Py) in lacustrine tight sandstone reservoirs. (N) Feldspar overgrowth (Feld-o) in lacustrine tight sandstone reservoirs. (O) Annhydrite (Anh) cementation in lacustrine tight sandstone reservoir. HV = high voltage; KV = kilovolt; MAG = magnification; SE = secondary electron; SEM = scanning electron microscope; WD = working distance.

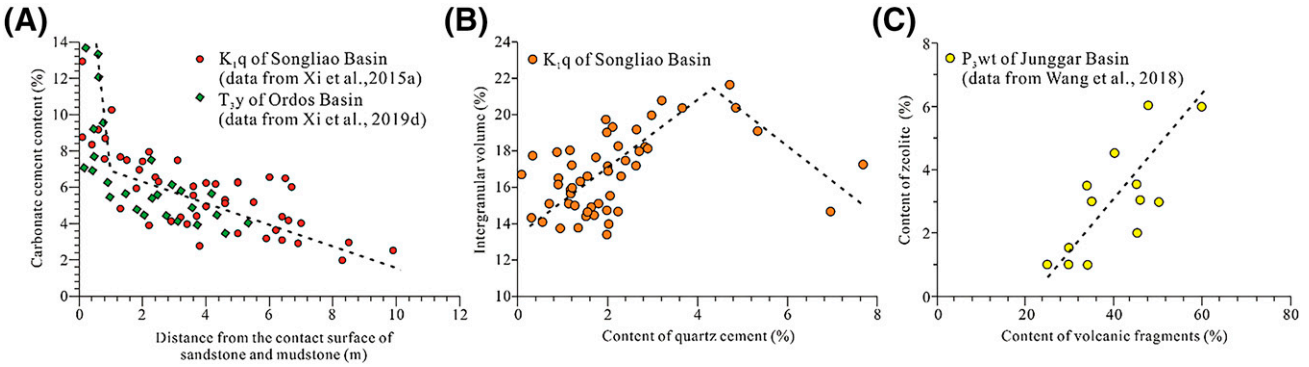

Figure 5. The major controlling factors of the key authigenic cements in tight sandstone reservoirs. (A) Relationship between distance from the sandstone–mudstone interface and carbonate cement content. (B) Relationship between quartz cement content and intergranular volume. (C) Relationship between volcanic fragment and zeolite content. The dashed line in each panel shows variation trends between the related parameters in the studied tight sandstone reservoirs (Xi et al., 2015a; Xi et al., 2019d). K_1q = Cretaceous Quantou Formation; P_3wt = Permian Wutonggou Formation; T_3y = Triassic Yanchang Formation.

cement content greater than 4%, authigenic quartz always occurred as pore-filling authigenic quartz (Figure 4F), and IGV decreased as quartz cement content increased (Figure 5B).

Zeolite Cementation

Zeolite in lacustrine tight sandstones is generally found in the form of analcite, heulandite, and laumontite. All of the zeolite types were observed to have developed in the Permian Jiamuhe Formation sandstone reservoirs of the Junggar Basin (Figure 4G, H); however, for parts of the Triassic Yanchang Formation sandstones, only laumontite was detected (Figure 4I). In the Jiamuhe Formation, analcite was replaced by heulandite (Figure 4G), indicating that analcite was formed at the earlier stage of diagenesis. Laumontite exhibited obvious cleavages and was partly dissolved in tight sandstones (Figure 4H, I). Analcite generally developed in the pore spaces where intermediate-acidic volcanic fragments were centered (Figure 4G), whereas laumontite consistently occurred in the sandstones abundant with intermediate-basic volcanic fragments (Figure 4H). For the tight sandstones of the Permian Jiamuhe Formation in the Junggar Basin, the content of zeolite cements increased with volcanic fragments (Figure 5C), implying that zeolite is mainly associated with volcanic materials.

Clay Minerals

Authigenic clay minerals were commonly observed in the pore spaces of the lacustrine sandstones. Clay minerals in the intergranular pores are able to divide larger pores into micropores, significantly decreasing the porosity and permeability of sandstone reservoirs (Wu et al., 2012; Wilson et al., 2014). Mixed-layer illite/smectite (I/S), illite, and chlorite were observed to have been extensively developed. Although kaolinite was also present in some of the relatively shallow burial tight sandstone intervals, the content was too low to have an impact on the reservoir quality. Mixed-layer I/S mainly distributed on the surface of volcanic rock fragments and occurred as flaky crystals, with illite making up more than 80% (Figure 4J). Filamentous illite generally formed in primary pores, seriously destroying the pores and pore throats (Figure 4K). Needle-shaped chlorite acted as a pore-lining authigenic clay mineral in most of the reservoirs studied (Figure 4L), and scattered chlorite flakes also performed a pore-filling role in the Triassic Yanchang Formation tight sandstones.

Other Minor Authigenic Minerals

Minor cements were also detected in the lacustrine tight sandstone reservoirs. Pyrite and feldspar overgrowth were commonly observed in all of the basins studied (Figure 4M, N), but the amounts were always less than 0.5%, which is too low to have a negative impact on the reservoir quality. In addition, anhydrite was found in several intervals of the Triassic Yanchang Formation in the Ordos Basin (Figure 4O). Other minor cements (i.e., siderite and dawsonite) were detected in the Cretaceous Quantou Formation

of the Songliao Basin. Although such minor cements have negligible effects on reservoir quality, they can generally act as an effective indicator in diagenetic environment evolution studies (Bjørlykke and Jahren, 2012).

Dissolution

Dissolution is the most important type of constructive diagenesis for reservoir quality. In the Cretaceous Quantou Formation in the Songliao Basin and Triassic Yanchang Formation in the Ordos Basin, dissolution generally is associated with detrital feldspars and volcanic rock fragments, resulting in the formation of a considerable number of secondary pores (Figure 6A–C). In contrast, the secondary pores formed via laumontite dissolution acted as the most important reservoir space in the Permian Jiamuhe Formation in the Junggar Basin (Figure 6D). Small amounts of laumontite dissolution pores were also detected in the Triassic Yanchang Formation in the Ordos Basin, but their distribution was limited (Figure 6E). Calcite cements were observed to be slightly dissolved in parts of the Cretaceous Quantou Formation in the Songliao Basin (Figure 6F). In general, silicate minerals, such as feldspars, volcanic rock fragments, and laumontite, in the studied lacustrine tight sandstone reservoirs were observed to have dissolved more extensively compared to the carbonate cements.

Oil Occurrence Characteristics

Oil emplacement can be regarded as a special diagenetic event in sandstone reservoirs (Xi et al., 2019c). The micro-occurrence of crude oil in the pore spaces influences the diagenetic alteration process and provides visual evidence allowing for the determination of the sequential order among diagenetic events and oil emplacement (Xi et al., 2015a). Based on fluorescence microscopy, crude oil was observed mostly in the primary pores, forming high oil saturations in

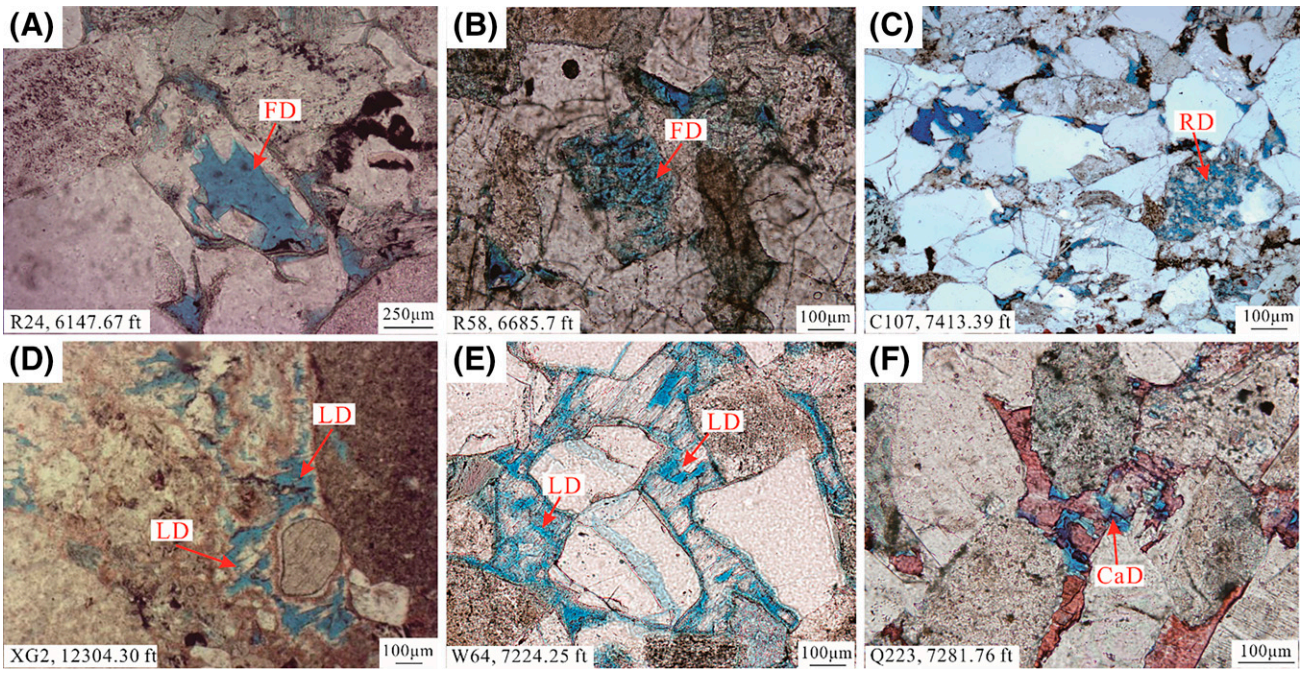

Figure 6. Dissolution characteristics in the lacustrine tight sandstone reservoirs of China. Sample number and depth labeled in lower left corners. (A, B) Feldspar dissolution (FD) in the Cretaceous Quantou Formation tight sandstone reservoirs of the Songliao Basin. (C) Rock fragment dissolution (RD) in the Triassic Yanchang Formation sandstone reservoirs of the Ordos Basin. (D) Laumontite dissolution (LD) in the Permian Jiamuhe Formation tight sandstone reservoirs of the Junggar Basin. (E) LD in the Triassic Yanchang Formation sandstone reservoirs of the Ordos Basin. (F) Calcite dissolution (CaD) in the Cretaceous Quantou Formation tight sandstone reservoirs of the Songliao Basin.

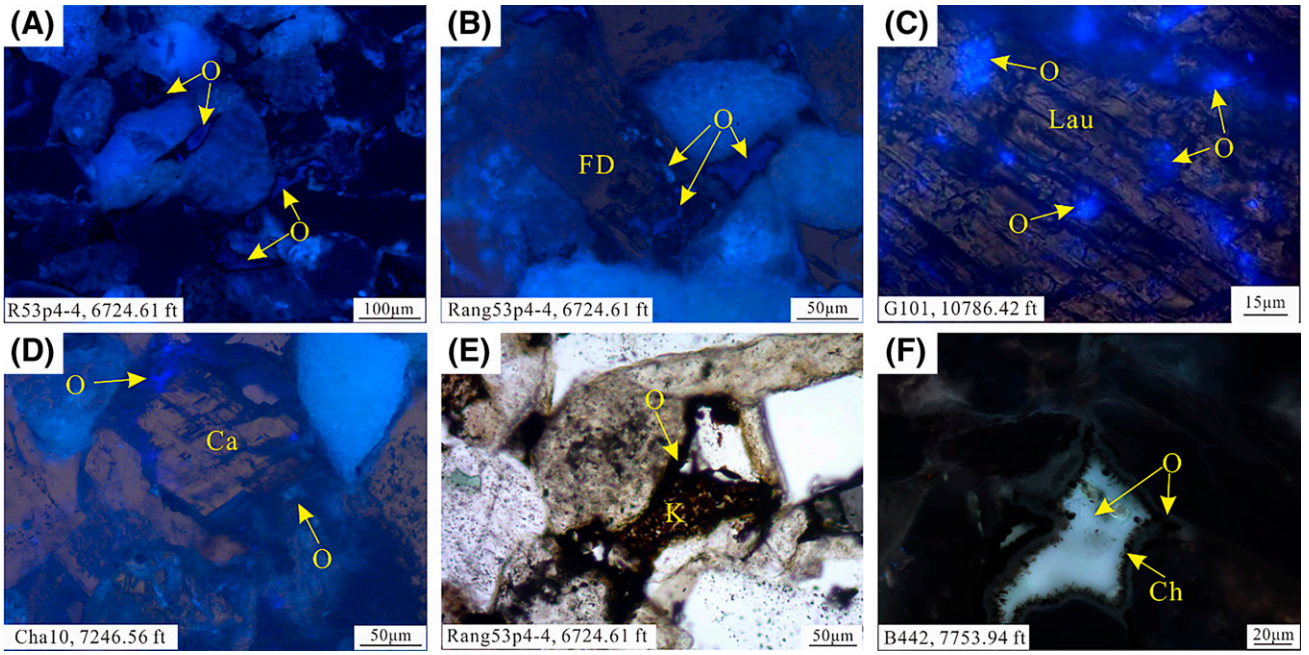

Figure 7. Oil (O) fluorescence observed in the lacustrine tight sandstone reservoirs. Sample number and depth labeled at lower left corners of the photomicrographs. (A) In the primary pores of the Cretaceous Quantou Formation. (B) In the primary and feldspar dissolution (FD) pores of the Cretaceous Quantou Formation (Xi et al., 2015a). (C) In the laumontite (Lau) dissolution pores of the Permian Jiamuhe Formation. (D) In the narrow gaps left by carbonate cementation of the Cretaceous Quantou Formation (Xi et al., 2015a). (E) In the micropores of authigenic kaolinite (K) of the Cretaceous Quantou Formation (Xi et al., 2015a). (F) In the chlorite (Ch)-coated primary pores of the Triassic Yanchang Formation. Ca = calcite.

the reservoirs dominated by primary pores (Figure 7A, B). In addition, oil was observed in intraparticle pores in detrital grains and authigenic mineral dissolution pores. For example, crude oil in feldspar dissolution pores of the Cretaceous Quantou Formation tight sandstones in the Songliao Basin (Figure 7B) indicate that oil emplacement occurred before feldspar dissolution. In the Permian Jiamuhe Formation tight sandstone reservoirs of the Junggar Basin, laumontite dissolution pores were filled by crude oil (Figure 7C), suggesting that laumontite dissolution principally occurred before oil emplacement. The presence of oil was also connected with the precipitation of authigenic minerals. In the Cretaceous Quantou Formation of the Songliao Basin, oil was observed in the narrow gaps left by calcite cementation (Figure 7D), and micropores located between authigenic kaolinite crystals were also filled by crude oil (Figure 7E). Furthermore, chlorite coatings were detected to have commonly developed in the Triassic Yanchang Formation of the Ordos Basin (Chen et al., 2017; Xi et al., 2019c), and oil emplacement inhibited any further growth via the charging into primary pores and intergranular micropores (Figure 7F).

DISCUSSION

Evolution History of Diagenesis and Oil Emplacement

An integrated diagenetic sequence is essential for the in-depth study of the porosity evolution in sandstone reservoirs (Xi et al., 2015a; Lai et al., 2018). Paragenetic sequences of diagenesis and oil emplacement can be established by synthesizing petrographic evidence, fluid inclusion measurements, and the analysis of mineral paragenesis. In the following, the procedures of diagenetic sequence analysis are discussed in detail, using the tight sandstones of the Cretaceous Quantou Formation in the Songliao Basin as an example.

Paragenesis of Authigenic Minerals

The major diagenetic events in the Cretaceous Quantou Formation include compaction, quartz cementation, calcite cementation, feldspar dissolution, and minor cements from feldspar overgrowth, ferrocalcite, and ankerite (Figure 8A–F). The relationships between these diagenetic minerals, including authigenic mineral

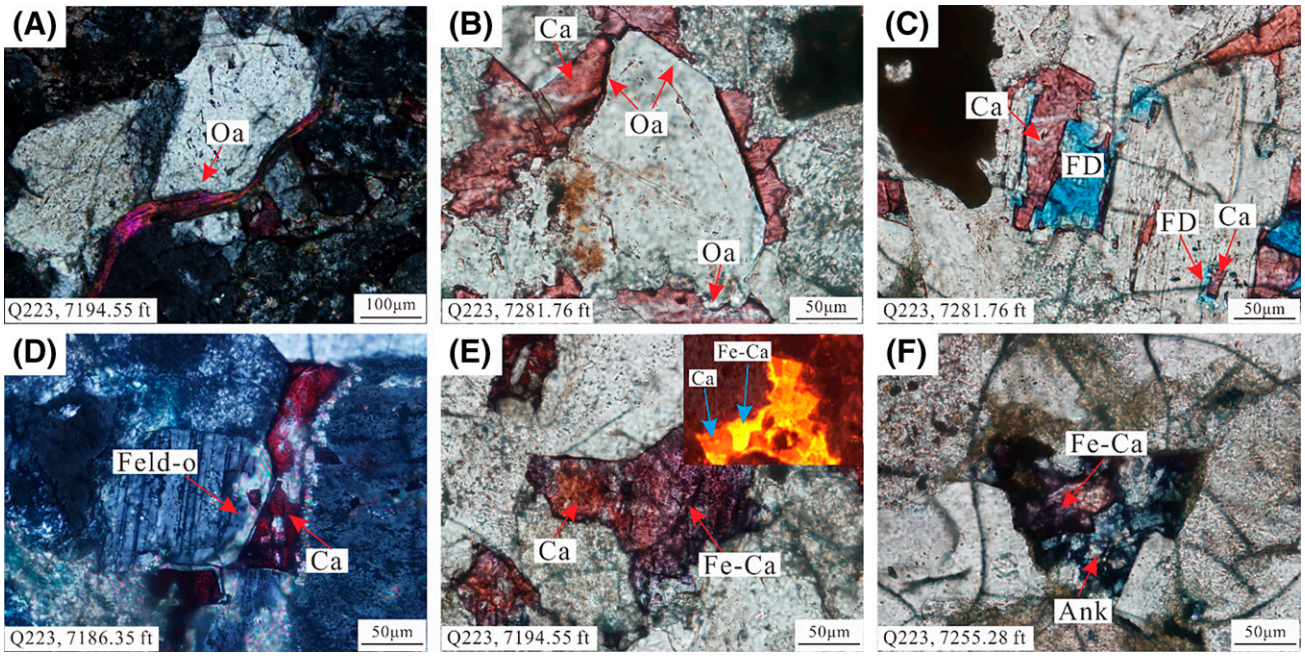

Figure 8. Petrographic evidence on the relationships between the diagenetic minerals in the Cretaceous Quantou Formation tight sandstone reservoirs of the Songliao Basin. Sample number and depth labeled at the lower left corners of the photomicrographs. (A) Quartz overgrowth (Oa) and mica deformation. (B) Oa and calcite (Ca) cements. (C) Feldspar dissolution (FD) pores filled by Ca cement. (D) Feldspar overgrowth (Feld-o) replaced by Ca cement. (E) Ca cement replaced by ferrocalcite (Fe-Ca). (F) Fe-Ca replaced by ankerite (Ank).

crosscutting and mineral dissolution filling, allow us to directly determine the sequential order of each diagenetic event. More specifically, large formations of quartz overgrowths were observed, whereas surrounding ductile mica was seen to be strongly deformed due to mechanical compaction (Figure 8A). This indicates that quartz cementation occurred during the early diagenetic stage, with weak compaction. Calcite cements developed in the pores that remained from the quartz cementation and subsequently replaced the quartz overgrowth (Figure 8B). Calcite cements were also detected in feldspar dissolution pores (Figure 8C). These observations suggest that calcite precipitation principally occurred after quartz cementation and feldspar dissolution. In addition, feldspar overgrowths were replaced by calcite cements (Figure 8D), indicating that feldspar overgrowth took place earlier than calcite cementation. Among the carbonate cements, ferrocalcite replaced the calcite (Figure 8E) and was subsequently replaced by ankerite (Figure 8F). This suggests that the precipitation order of carbonate cements was as follows: calcite, ferrocalcite, and ankerite. Thus, a preliminary diagenetic sequence in the Cretaceous Quantou Formation tight sandstone reservoirs can be described as compaction, feldspar dissolution, quartz cementation, calcite cementation, ferrocalcite formation, and ankerite precipitation.

Fluid Inclusion and Oxygen Isotope Analysis

Petrographic evidence provides a relative sequence order of each diagenetic process. The diagenetic sequence can be evaluated further by investigating the formation temperature of the major authigenic minerals in sandstone reservoirs (Cao et al., 2018). Moreover, the homogenization temperature of fluid inclusions can effectively determine the precipitation time of several authigenic minerals, such as quartz overgrowth, carbonate cements, and zeolite (Robinson and Gluyas, 1992). In addition, oxygen isotopes can be used to calculate the formation temperature of authigenic minerals, including several clay minerals (Xi et al., 2019a). In the Cretaceous Quantou Formation tight sandstones, the homogenization temperatures of the fluid inclusions in the quartz overgrowth were generally in the range of 70°C to 90°C, which was lower than that of the calcite cements, varying from 90°C to 110°C (Figure 9). The number of fluid inclusion temperatures determined in the calcite cements was much lower than that of the quartz overgrowth. Thus, the temperature

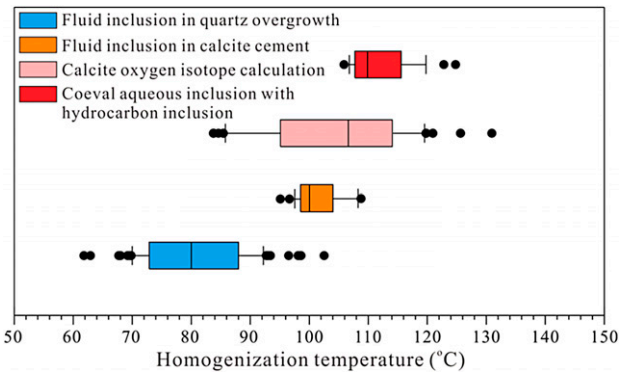

Figure 9. The homogenization temperature of fluid inclusions in quartz overgrowth, calcite cements, and hydrocarbon coeval aqueous inclusions in the Cretaceous Quantou Formation tight sandstone reservoirs.

derived from the oxygen isotopes may be able to overcome the data deficiencies associated with the carbonate cements. Based on the calcite-water oxygen isotope fractionation equation (Friedman and O'Neil, 1977), the temperature for calcite cements was calculated via the values of oxygen isotopes (Xi et al., 2015a). The results reveal a precipitation temperature of calcite within 95°C to 115°C. This range agrees with the homogenization temperature derived from the fluid inclusions (Figure 9). With the exception of the quartz overgrowth and calcite cement fluid inclusions, the hydrocarbon inclusions generally developed in the microfractures of the detrital quartz grains. The oil emplacement temperature in the Cretaceous Quantou Formation tight sandstone reservoirs can be used to estimate the homogenization temperature of the coeval aqueous inclusions (Dong et al., 2014). Microthermometry analysis revealed that the homogenization temperature of hydrocarbon coeval aqueous inclusions lay within 108°C to 116°C (Figure 9). This corresponds to the later stage of calcite cementation. Thus, the analysis also confirmed that the onset of the quartz overgrowth occurred before the initiation of calcite cementation, whereas oil emplacement took place during the later stage of calcite cementation.

Diagenetic Mineral Transformation Reactions

Although petrographic evidence and fluid inclusion analysis is able to establish the sequential order of major diagenetic events, the formation time of clay minerals and other minor cements is difficult to determine based solely on petrographic analysis. In addition, authigenic clays have a significant influence on the properties of reservoirs (Wilson et al., 2014). Thus, a more comprehensive diagenetic sequence that includes major diagenetic events and their paragenetic clay minerals is essential for research on sandstone reservoir. Previous studies have investigated the diagenetic mineral transformation reactions to clarify the authigenic mineral formation mechanisms of the Cretaceous Quantou Formation sandstones in Songliao Basin (Xi et al., 2015a, 2019b). Kaolinite and small amounts of microquartz cement were generated from K-feldspar dissolution (Figure 10A), and albitization of K-feldspar occurred during this process as well (Figure 10B). These indicate that K-feldspar dissolution occurred slightly earlier than the formation of kaolinite, albite, and microquartz cement. In the Cretaceous Quantou Formation sandstones, volcanic rock fragments can easily transform to smectite during the earlier stage of diagenesis. As the burial depth and temperature increased, smectite was observed to quickly transform into an ordered mixed-layer I/S or illite via random mixed-layer I/S (Cama et al., 2000). Moreover, excess silica was produced during the smectite-to-illite reactions, being a potential source for authigenic quartz (Figure 10C, D). Thus, smectite, kaolinite, and random mixed-layer I/S formed before the major precipitation stage of authigenic quartz, whereas ordered I/S, fabric illite, and flake chlorite were accompanied mainly by quartz cementation.

Diagenetic Sequence and Oil Emplacement Time

The fusion of petrographic evidence, fluid inclusion analysis, and diagenetic mineral transformation reactions allows for the establishment of an integrated paragenetic sequence of diagenesis for tight sandstone reservoirs (Figure 11). At the early burial stage, the diagenesis of tight sandstone reservoirs includes the following processes (from earliest to latest): compaction, smectite formation, random mixed-layer I/S transformation, K-feldspar dissolution, albitization, and kaolinite precipitation. Then, smectite and random mixed-layer I/S were extensively transformed to ordered mixed-layer I/S or discrete illite and chlorite, accompanied by the precipitation of quartz overgrowth. The calcite cements related to organic carbon occurred mainly for temperatures within 95°C to 115°C (Xi et al., 2015a). At even higher temperatures, a proportion of the calcite cements were replaced by ferrocalcite and ankerite. Moreover, based on the oil presence characteristics

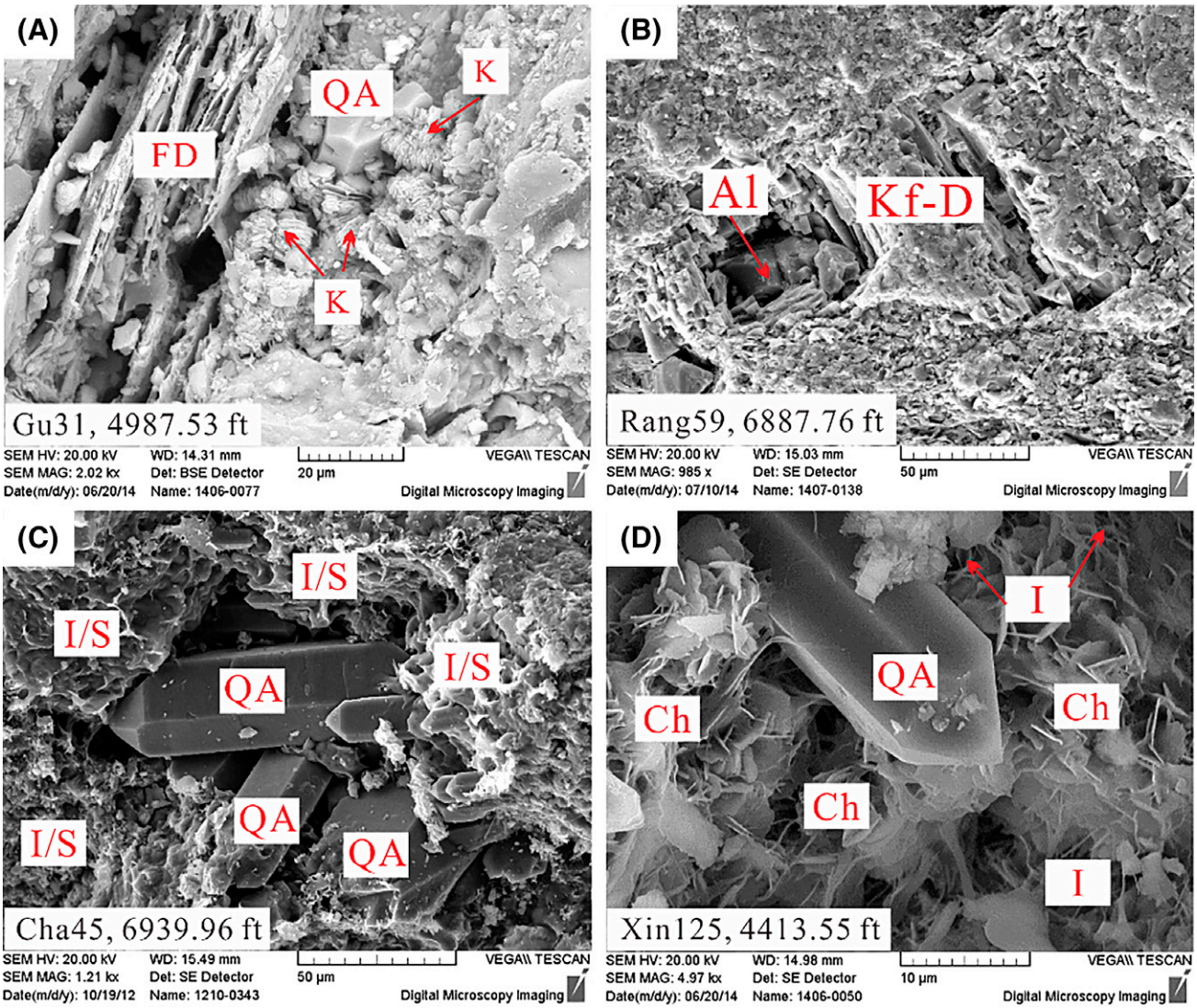

Figure 10. Authigenic minerals and petrographic characteristics used for the paragenesis interpretation shown in Figure 11 (Xi et al., 2015a). Sample number and depth labeled at the lower left corners of the photomicrographs. (A) K-feldspar dissolution (Kf-D) accompanied by kaolinite (K) and microquartz precipitation. (B) K-feldspar dissolution and albitization. (C) Mixed-layer illite/smectite (I/S) accompanied by quartz (QA) cementation. (D) Illite (I) and chlorite (Ch) accompanied by authigenic QA. Al = albite; BSE = backscattered electron; FD = feldspar dissolution.

and microthermometry analysis of hydrocarbon inclusions, oil emplacement during the later stage of calcite cementation was also added to the diagenetic evolution sequence (Figure 11).

Quantitative Analysis on Reservoir Porosity Evolution

Quantitative studies on porosity evolution are key for the evaluation of reservoir quality and the prediction of oil exploration fairways in tight sandstone reservoirs. By applying the paragenetic sequence of diagenesis, we propose a method to recover the porosity evolution process across geological time (or paleoburial depth). The proposed method is described in this section, using the example of well R59, 2119.78 m (6954.66 ft), from the Cretaceous Quantou Formation tight sandstones of the southwestern Songliao Basin.

Initial Sandstone Porosity

Initial porosity refers to the ratio of pore volume in the newly deposited sediments just before burial and compaction began. As the starting point of porosity evolution recovery, initial porosity significantly influences

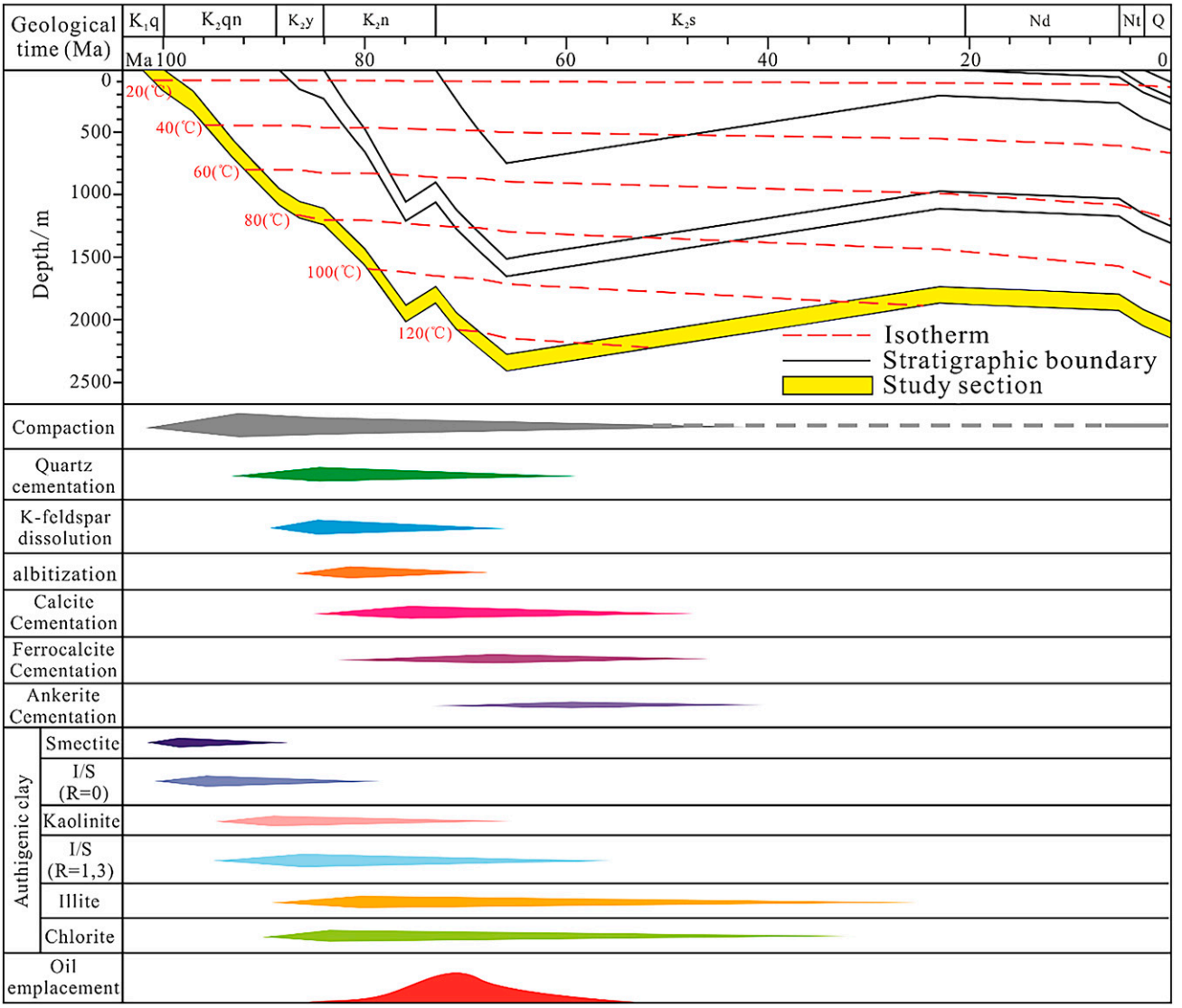

Figure 11. The paragenetic sequence of diagenesis and oil emplacement in the Cretaceous Quantou Formation tight sandstone reservoir (modified from Xi et al., 2015a). I/S = illite/smectite; K_1q = Quantou Formation; K_2n = Nenjiang Formation; K_2qn = Qingshankou Formation; K_2s = Sifangtai Formation; K_2y = Yian Formation; Nd = Daan Formation; Nt = Taikang Formation; Q = Quaternary.

the accuracy of porosity evolution studies. The initial porosity of sediments is principally controlled by texture parameters, including grain size, sorting, and sphericity (Beard and Weyl, 1973). Previous studies have made progress in determining the initial porosity of sandstone via empirical statistics, the extension of the porosity trend line, and simulation experiments (Gluyas and Cade, 1999; Xi et al., 2015b). Among these, the most commonly used method in the current literature is described as follows (Beard and Weyl, 1973).

$$\Phi_0 = 20.91 + 22.90/So \quad (1)$$

where Φ_0 is initial porosity (%) and So is the Trask sorting coefficient.

Based on this, a new model concerning average grain size and So was proposed to calculate initial porosity according to the diagenetic simulation experiment on sandstones with different texture parameters (Xi et al., 2015b).

$$\Phi_0 = -3.04So - 3.49M + 47.83 \quad (2)$$

where M is the average grain size (mm).

For the well-sorted medium-coarse sandstones, equations 1 and 2 are similar. For moderate-sorted

fine-medium sandstones, however, in equation 1, the initial porosity is much smaller than the commonly assumed value of 40% (Houseknecht, 1987; Lundegard, 1992). Based on rock texture parameter analysis (Xi et al., 2015a), equation 2 was used to calculate the initial porosity of the Cretaceous Quantou Formation sandstone sample of well R59, 2119.78 m (6954.66 ft) (Table 2), obtaining a value of 38.91%.

Table 2. The Composition, Grain Size, and Sorting Coefficient of the Sample R59, 2119.78 m (6954.66 ft)

Rock Composition, %			Sorting Coefficient	Average Grain Size, mm
Quartz	Feldspar	Rock fragment		
41.56	27.3	31.14	2.59	0.3

Paleoburial Depth (or Time) with Respect to Key Diagenetic Events

To establish the porosity evolution process from deposited sediments to present tight sandstones, time (or paleoburial depth) of the major diagenesis needs to be determined. Compaction occurred during the whole burial process; hence, the time (or paleoburial depth) at which cementation and dissolution took place should be the most important issue to solve. First, the precipitation temperatures of the major cements were derived based on fluid inclusion microthermometry analysis and oxygen isotope temperature calculations (Figure 9). The corresponding time and paleoburial depth were then determined by combining the burial and thermal evolution history (Figure 12). For example, in well R59, in the tight sandstone sample at 2119.78 m (6954.66 ft) from the Cretaceous Quantou Formation, calcite cementation generally developed at 81.5 Ma, which corresponds to a depth of 1480 m (4855.64 ft). Furthermore, quartz cement began to form at 84.2 Ma, corresponding to a depth of 1240 m (4068.24 ft) (Figure 12). Feldspar dissolution temperature can be estimated using the formation of by-products kaolinite and microquartz overgrowths (Xi et al., 2015a), which, in our example, generally began at 89.0 Ma, corresponding to a depth of 1050 m (3444.88 ft) (Figure 12). In addition, the oil emplacement occurred mainly during the late stage of diagenesis, at 78 Ma, which corresponds to a depth of 1765 m (5790.68 ft) (Figure 12).

Contribution of Key Diagenesis to Thin Section Porosity

Based on thin section observation and image analysis, the contribution of the major diagenetic events, including quartz cement, calcite cements, and feldspar dissolution to thin section porosity can be quantitatively captured (Figure 13). The procedures can be summarized as follows: (1) select the FOV and mosaic image to represent the characteristics of the studied sample (Figure 13A); (2) manually identify the sandstone rock components in the mosaic image and quantify the area percentage of each major diagenetic event (Figure 13B, C); and (3) successively recover the pore space distribution characteristics at each key stage on the diagenetic sequence constraint (Figure 13D–F). For example, feldspar dissolution, quartz cementation, and calcite cementation are three types of volumetrically predominant diagenesis in the tight sandstone sample of well R59, 2119.78 m (6954.66 ft) (Figure 13). Feldspar dissolution improved the thin section porosity by approximately 0.69%, and quartz cementation and calcite cementation destroyed the thin section porosity by approximately 0.83% and 6.2%, respectively.

Relationship between Thin Section and Helium Porosity

The area percentage of each major diagenesis in thin section images is able to reflect its contribution to reservoir quality. However, it represents only two-dimensional characteristics, whereas the volume ratio in three dimensions is overlooked. There are always certain amounts of micropores that exist in tight sandstone reservoirs. These micropores developed mainly between authigenic clay minerals, and they were difficult to calculate in the two-dimensional area percentage through the microscope. For the helium porosity, however, the micropores could be measured easily, resulting in the differences between thin section and helium porosity. Thus, for a more accurate porosity evolution recovery, the two-dimensional area percentage is converted to volume ratio. The helium porosity was measured on more than 200 tight sandstone samples from the Cretaceous Quantou Formation. Among these, 40 samples with helium porosity within 0.2% to 10% were chosen to analyze the thin section porosity. The thin section and helium porosities were related exponentially (Figure 14).

$$y = 2.5169\ ln(x) + 4.1197,\ R^2 = 0.913 \qquad (3)$$

where x is the thin section porosity representing the two-dimensional area percentage, y is the helium

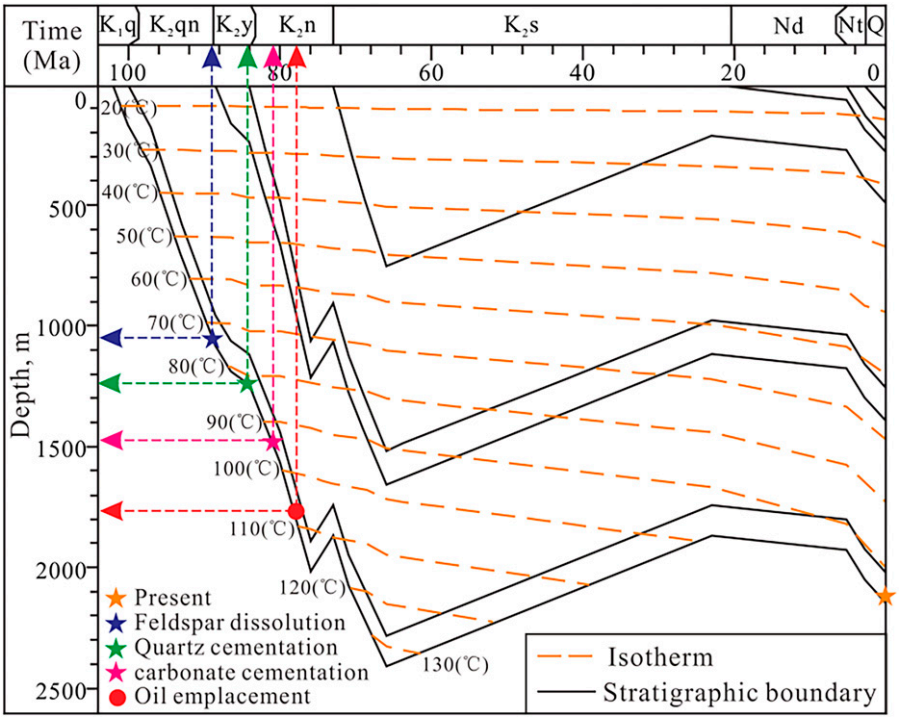

Figure 12. Time of occurrence and corresponding paleoburial depth of the major diagenesis processes in the Cretaceous Quantou Formation tight sandstone reservoirs. K_1q = Quantou Formation; K_2n = Nenjiang Formation; K_2qn = Qingshankou Formation; K_2s = Sifangtai Formation; K_2y = Yian Formation; Nd = Daan Formation; Nt = Taikang Formation; Q = Quaternary.

porosity representing the three-dimensional volume ratio, and R^2 is coefficient of determination.

The contribution of the major diagenesis on volume ratio can be approximated via the determined area percentage from the thin section image using the exponential relationship between thin section porosity and helium porosity. Results showed that the feldspar dissolution improved thin section porosity of approximately 0.69% can be converted to a helium porosity of approximately 3.19%, and the quartz cementation and calcite cementation–destroyed thin section porosities of approximately 6.2% and 0.83% can be converted to helium porosities of approximately 8.72% and 3.65%, respectively (Table 2).

Porosity Evolution Trends Caused by Mechanical Compaction

Mechanical compaction is the most important controlling factor for porosity loss in tight sandstone reservoirs (Bjørlykke, 2014). Previous studies attribute the porosity loss caused by compaction to the early stage of the diagenetic sequence (Wei et al., 2016). However, mechanical compaction in the tight sandstones occurred during the entire diagenetic processes. Thus, to accurately determine porosity evolution, it is essential to assign the total porosity loss caused by mechanical compaction into each diagenetic stage.

First, the porosity evolution trend caused only by mechanical compaction needs to be established for the studied areas. The sandstones that experienced normal mechanical compaction (without pressure abnormity) comply with the following conditions: (1) the samples exhibit a normal formation fluid pressure, (2) the samples do not contain authigenic cements, and (3) the sample minerals have not undergone dissolution (Cao et al., 2018). Based on these conditions, several samples were chosen at shallow to deep burial depths in the studied areas. The analyzed samples exhibited a similar composition and grain size, whereas the *So* was distributed over a relatively wide range (1.5–2.0) (Xi et al., 2015a, b). Porosity evolution curves versus burial depth (normal compaction curve [NCC]) were established for samples with different So (Figure 15A). According to the diagenesis paragenetic sequence, porosity loss before quartz cementation was caused exclusively by mechanical compaction (Figure 15B). Thus, the porosity evolution at this stage can be estimated from the

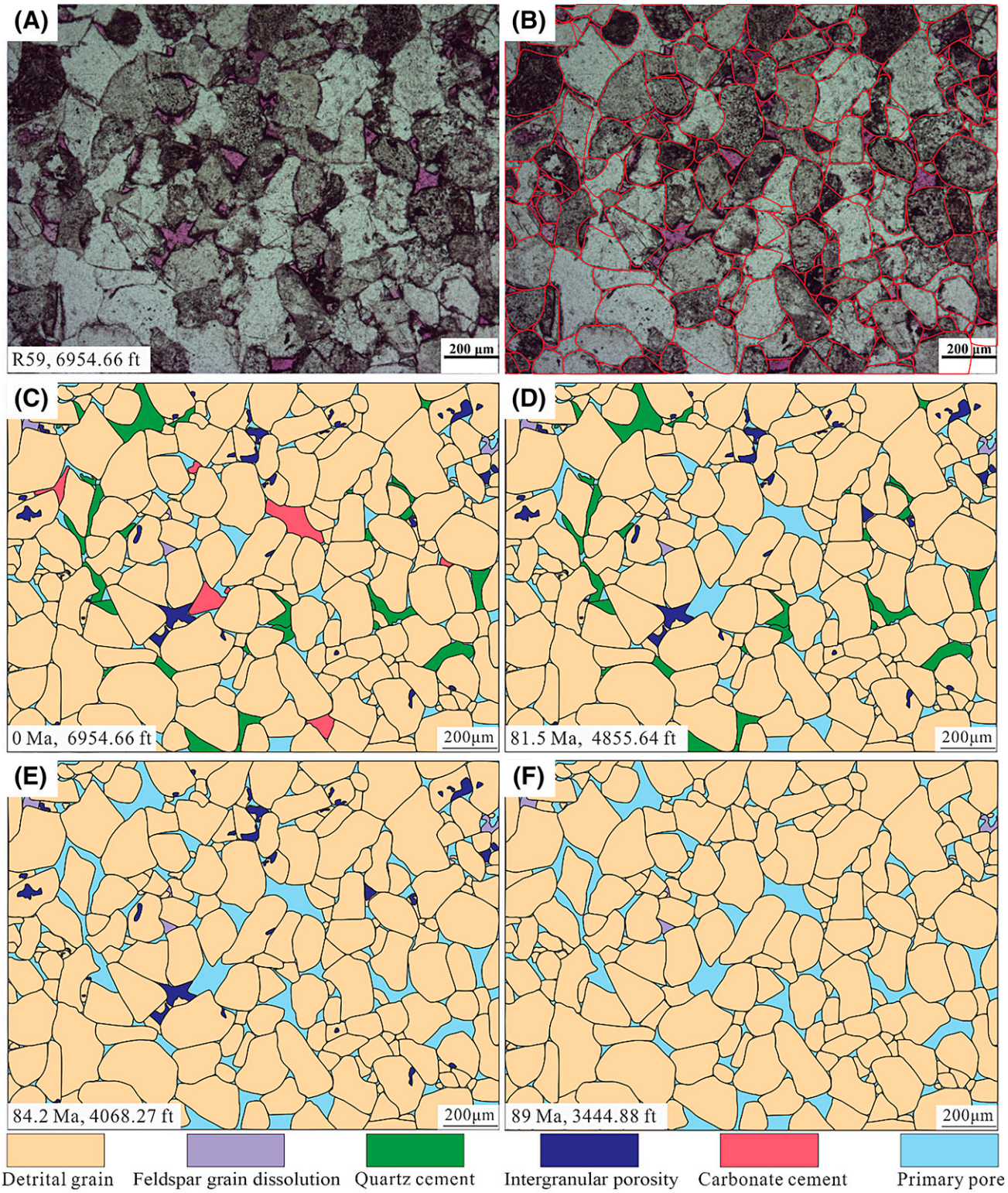

Figure 13. Schematic illustration of sequential diagenetic events at selected time increments (0–89 Ma) based on petrographic analysis of tight sandstone from well R59. (A) Photomicrograph, plane polarized light. (B) Image segmentation of grain boundaries (red lines). (C) Initial primary intergranular porosity (blue). (D) Before carbonate cementation (red). (E) Before quartz cementation (green). (F) Before feldspar grain dissolution (purple).

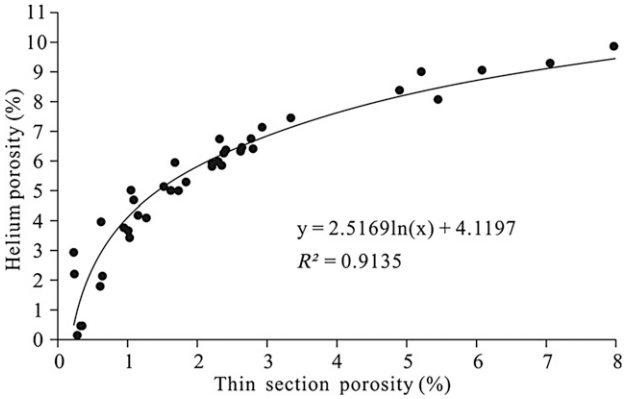

Figure 14. Relationship between thin section porosity and helium porosity in the Cretaceous Quantou Formation. R^2 = coefficient of determination.

corresponding NCC curves under constraint of sorting coefficients. Following quartz cementation, majority of the detrital quartz grains developed overgrowths, which strengthened the stress resistance capacity of the sandstone reservoirs. Consequently, porosity loss did not obey the NCC. In this case, the porosity loss caused by mechanical compaction during each diagenetic stage was determined via the porosity loss ratio of the NCC at each burial depth interval. Finally, the total porosity loss caused by mechanical compaction was assigned to corresponding diagenetic periods, and a more accurate porosity evolution process across geologic time was reconstructed (Figure 15B).

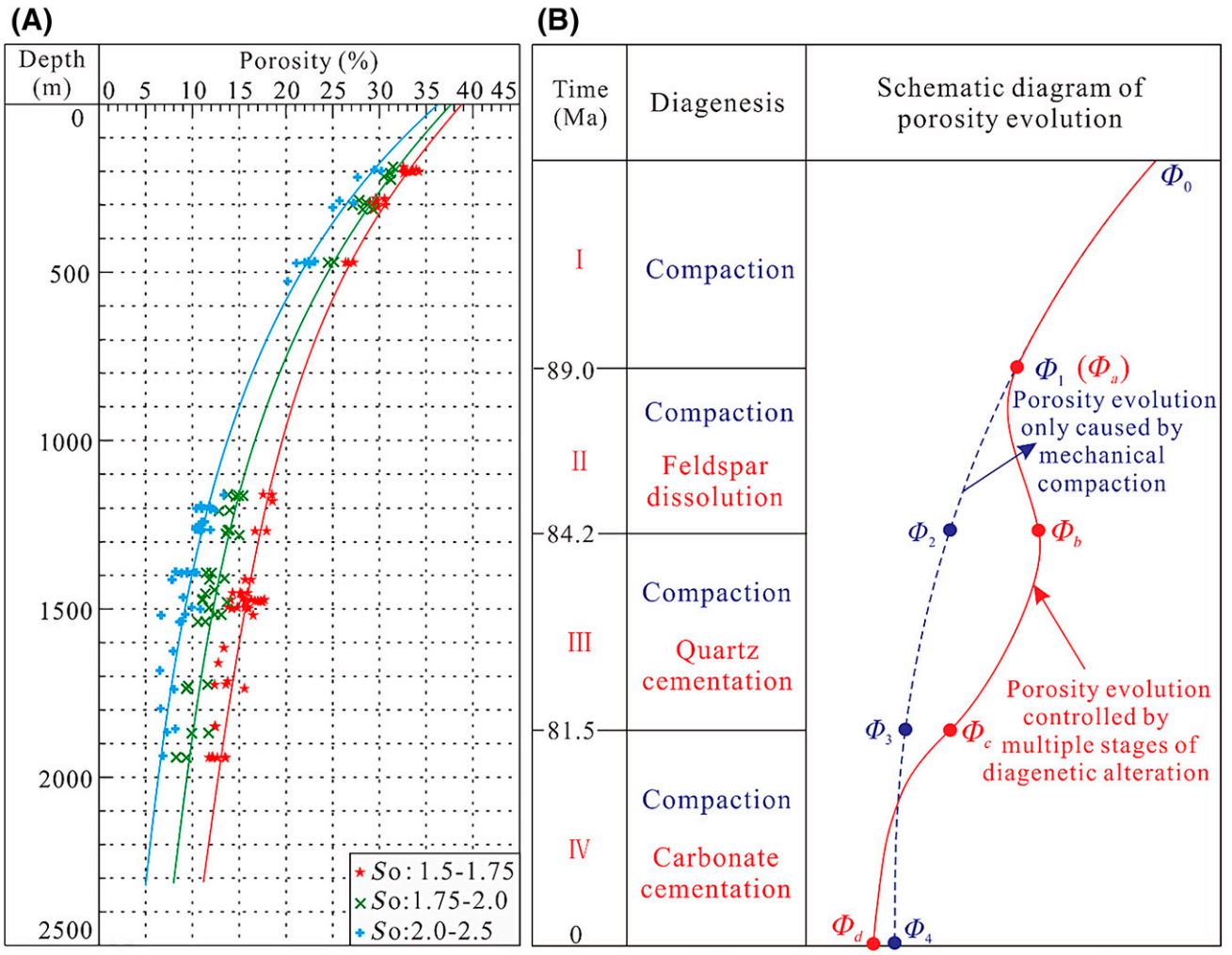

Figure 15. (A) Porosity evolution trends of the Cretaceous Quantou Formation tight sandstones with different Trask sorting coefficients (*So*), showing that the samples only encounter mechanical compaction. (B) Schematic diagram of the porosity evolution processes controlled by multiple stages of diagenetic alterations in sandstone reservoirs. Φ_a, Φ_b, Φ_c, and Φ_d = porosities at the beginning or end of each key diagenetic event in the porosity evolution curve after mechanical compaction; Φ_1, Φ_2, Φ_3, and Φ_4 = porosities at the beginning or end of each key diagenetic event in the normal compaction curve.

The Φ_a, Φ_b, Φ_c, and Φ_d are the porosities at the beginning or end of each key diagenetic event in the porosity evolution curve after mechanical compaction, and Φ_1, Φ_2, Φ_3, and Φ_4 are the porosities at the beginning or end of each key diagenetic event in the NCC. Before quartz cementation, the porosity loss caused by mechanical compaction can be obtained directly from NCC. Thus, from Figure 15B we have the following.

$$\Phi_a = \Phi_1 = \Phi_0 - \Phi_{(0-1)mc} \quad (4)$$

$$\Phi_b = \Phi_2 + \Phi_{fd} = \Phi_0 - \Phi_{(0-1)mc} - \Phi_{(1-2)mc} + \Phi_{fd} \quad (5)$$

where Φ_0 is the initial porosity, Φ_{fd} is the porosity improved by feldspar dissolution, $\Phi_{(0-1)mc}$ represents the porosity loss caused by compaction during diagenetic stage I (Figure 15B), and $\Phi_{(1-2)mc}$ represents the porosity loss caused by compaction during diagenetic stage II (Figure 15B).

Following quartz cementation, the total porosity loss caused by mechanical compaction $\Phi_{(2-4)c}$ can be expressed as follows.

$$\Phi_{(2-4)c} = \Phi_{tc} - \Phi_{(0-1)mc} - \Phi_{(1-2)mc} \quad (6)$$

where Φ_{tc} represents the total porosity loss caused by mechanical compaction in the entire burial process, and can be calculated as follows.

$$\Phi_{tc} = \Phi_0 - \Phi_{qc} - \Phi_{cc} - \Phi_p + \Phi_{fd} \quad (7)$$

where Φ_{qc} is the porosity loss caused by quartz cementation, Φ_{cc} is the porosity loss caused by carbonate cementation, and Φ_p is the present porosity.

Thus, the porosity loss caused by compaction during diagenetic stages III and IV can be determined according to the porosity loss ratio in the NCC at each burial depth interval as follows.

$$\Phi_{(2-3)mc} = [(\Phi_3 - \Phi_2)/(\Phi_4 - \Phi_2)] \times \Phi_{(2-4)mc} \quad (8)$$

$$\Phi_{(3-4)mc} = [(\Phi_4 - \Phi_3)/(\Phi_4 - \Phi_2)] \times \Phi_{(2-4)mc} \quad (9)$$

where $\Phi_{(2-3)mc}$ represents the porosity loss caused by compaction during diagenetic stage III and $\Phi_{(3-4)mc}$ represents the porosity loss caused by compaction during diagenetic stage IV (Figure 15B).

Finally, Φ_c and Φ_d can be calculated by equations 10 and 11.

$$\Phi_c = \Phi_b - \Phi_{qc} - \Phi_{(2-3)mc} \quad (10)$$

$$\Phi_d = \Phi_c - \Phi_{cc} - \Phi_{(3-4)mc} \quad (11)$$

Porosity Evolution Controlled by Multiple Stages of Diagenetic Alterations

Based on the above analysis of the porosity loss caused by compaction, porosity evolution trends for the well R59, 2119.78 m (6954.66 ft), sample were calculated at burial depths corresponding to the beginning or end of major diagenetic events (Table 3). The porosity evolution process for the well R59, 2119.78 m (6954.66 ft), sample was then established using the volumetrically predominant diagenetic events (Figure 16). Results show that mechanical compaction was the leading cause of porosity loss in the Cretaceous Quantou Formation. The feldspar dissolution content was too low to induce significant reservoir porosity improvement. Following quartz cementation, the reservoir was tight, and calcite cementation further lost the sandstone porosity and permeability.

Integration of Reservoir Porosity Evolution and Oil Emplacement

The porosity at the time of oil emplacement can be used to effectively evaluate the reservoir potential of tight sandstone in oil exploration studies. Based on the diagenesis characteristics and diagenetic sequence, an integration of porosity evolution and oil emplacement can be established. Based on this, information on burial history and diagenetic sequences, formation time of tight reservoirs and related mechanisms, and the time of oil emplacement during the porosity evolution process can be determined. Three typical tight sandstone reservoirs were chosen as examples to illustrate the integration of diagenesis, porosity evolution, and oil emplacement according to diagenetic differences in the sandstones from the lacustrine oil-bearing basins in the east to west of China.

Example 1: Tight Sandstone Reservoirs of the Cretaceous Quantou Formation in the Songliao Basin, Northeastern China

Based on the detailed methods and procedures in the sections Evolution History of Diagenesis and Oil Emplacement and Quantitative Analysis on Reservoir Porosity Evolution, the integration of diagenesis, average porosity evolution, and oil emplacement across

Table 3. Quantitative Studies on Porosity Evolution versus Geologic Time (or Paleoburial Depth) of the Sample R59, 2119.78 m (6954.66 ft)

Diagenetic Event	Time, Ma	Paleodepth, m	Diagenesis Control on Thin Section Porosity, %	Diagenesis Control on Helium Porosity, %	Porosity Loss Caused by Compaction, %	Porosity Evolution without Compaction Calibration, %	Actual Porosity Evolution, %
Sediments deposition	102	0	0	0	0	38.91	38.91
Feldspar dissolution	89	1050 (3444.88 ft)	+0.69	+3.19	−19.71	16.97	19.2
Quartz cementation	84.2	1240 (4068.24 ft)	−6.2	−8.72	−1.3	20.16	21.09
Calcite cementation	81.5	1480 (4855.64 ft)	−0.83	−3.65	−0.46	11.45	11.92
Present	0	2119.78 (6954.66 ft)	/	/	−0.47	7.8	7.8

+ = porosity improvement; − = porosity loss; / = no data.

geologic time was established in the Cretaceous Quantou Formation tight sandstone reservoirs. Compaction dominated more than 60% of total porosity loss in the tight sandstones (Xi et al., 2015a). Quartz cementation was relatively strong in the Cretaceous Quantou Formation compared to the other two study areas. After compaction, quartz cementation occurred, along with the filling of clay minerals, and the average porosity of the sandstone reservoirs fell below 10%. Although feldspar dissolution increased reservoir porosity, the dissolution pore content was too low to improve significant reservoir quality. This indicates that mechanical compaction is dominant in the reduction of sandstone reservoir porosity, and the formation of tight sandstone reservoirs is ultimately determined by quartz cementation. The analysis of porosity evolution and oil charging time demonstrated that oil emplacement generally occurred following tight sandstone formation in the Cretaceous Quantou Formation of the Songliao Basin. Under these conditions, oil charging becomes difficult and oil saturation is consistently low in these sandstone reservoirs, suggesting that more attention should be placed on the oil emplacement mechanism in exploration studies of this type of tight sandstone oil reservoir.

Example 2: Tight Sandstone Reservoirs of the Triassic Yanchang Formation in the Ordos Basin, Central China

Diagenesis in the Triassic Yanchang Formation of the Ordos Basin generally includes compaction, quartz cementation, feldspar dissolution, albitization, and authigenic mineral cementation. Among these, compaction, calcite cementation, and chlorite cementation are the volumetrically predominant diagenesis types, whereas quartz cementation, feldspar dissolution, and other authigenic filling exert a relatively smaller influence on reservoir porosity (Xi et al., 2019c). The previous works demonstrate that compaction also accounted for 50% to 60% of total porosity loss (Xi et al., 2019d). After the cementation of quartz, the average porosity of sandstones was maintained at approximately 15%. Following the major calcite cementation process, the sandstone porosity decreased to less than 10%. Thus, the tight sandstone formation ultimately took place via calcite cementation. Previous studies have concluded that two stages of oil emplacement occurred in the studied sandstone reservoirs (Li et al., 2012). The inclusion of the porosity evolution process demonstrates that both of

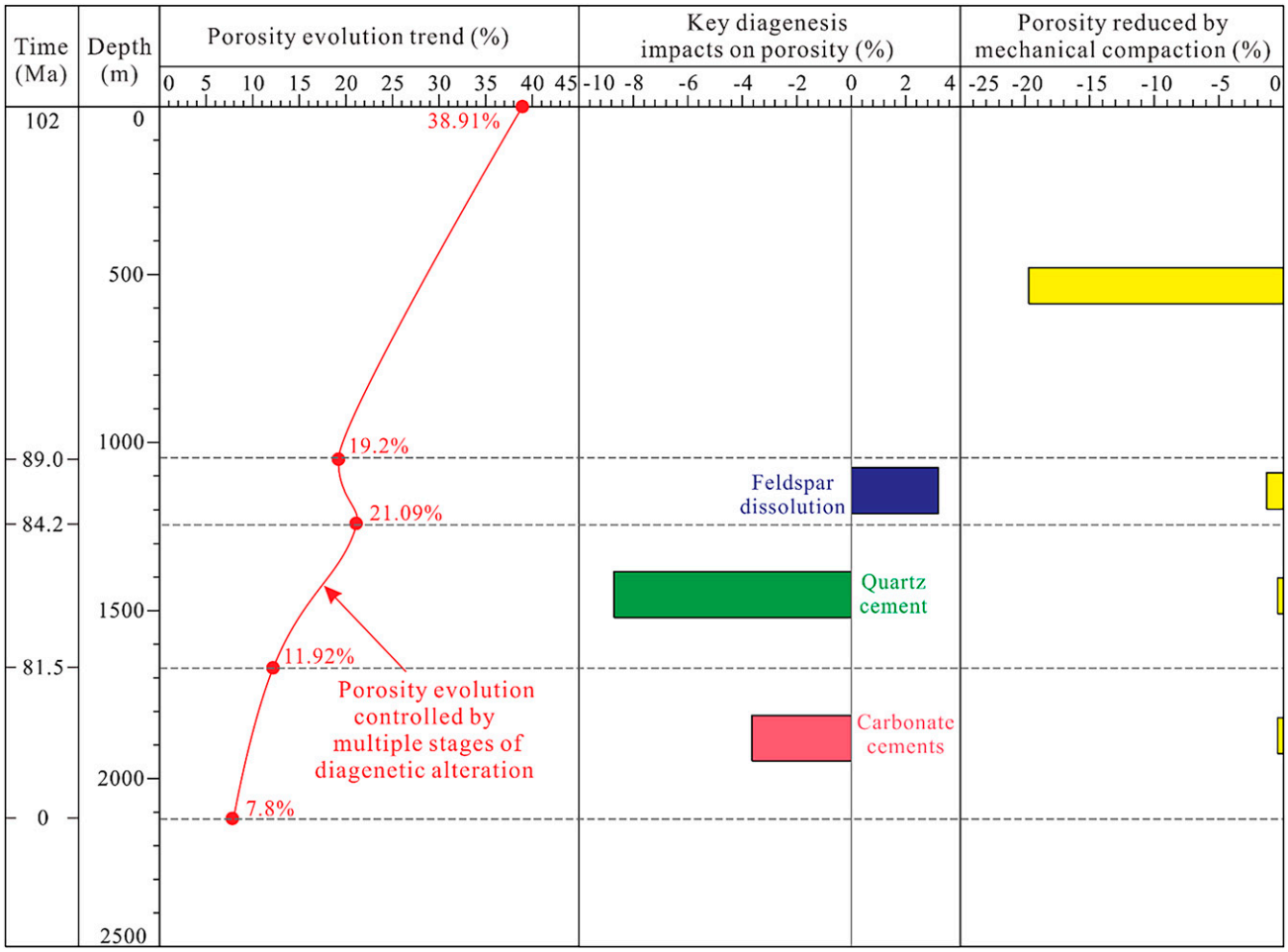

Figure 16. Diagenesis impacts on reservoir porosity and the evolutionary process of the tight sandstone sample of well R59, 2119.78 m (6954.66 ft), in the Cretaceous Quantou Formation.

the oil-charging stages occurred before tight sandstone formation. For this type of sandstone reservoir, oil charging primarily occurred while the reservoir properties may be called conventional, which is associated with relatively high oil saturation. Nevertheless, diagenetic alterations become more complicated in mixed water-oil pore fluid systems following oil emplacement (Kolchugin et al., 2016). Hence, the diagenetic evolution and sandstone densification process after oil accumulation should be regarded as a research hotspot in oil exploration studies for this type of tight sandstone.

Example 3: Tight Sandstone Reservoirs of the Permian Jiamuhe Formation in the Junggar Basin, Northwestern China

The characteristics of the diagenesis process in the Permian Jiamuhe Formation of the Junggar Basin are distinct from those of the Triassic Yanchang Formation of the Ordos Basin and the Cretaceous Quantou Formation of the Songliao Basin. This is attributed to the major differences in rock composition. With the exception of the similar diagenetic events related to compaction, quartz cementation, calcite cementation, and some clay mineral fillings, zeolite was the most important cement agent in the Permian Jiamuhe Formation, with sandstones abundant in volcanic rock fragments. Based on the comprehensive analysis on reservoir diagenesis, the diagenetic sequence was established for the Permian Jiamuhe Formation tight sandstone reservoirs (Yuan et al., 2017). This was subsequently combined with the quantitative recovery of the average porosity evolution, allowing for the clarification of sandstone porosity loss mechanisms. The porosity loss ratio caused by mechanical compaction was lower than the above

two sandstone reservoirs, which is a result of the enhanced pressure resistance by zeolite cementation. Zeolite cementation rapidly decreased the average porosity of the sandstone reservoirs to below 10%, leading to the formation of tight sandstones in the Permian Jiamuhe Formation. Following this, tectonic movement resulted in the uplifting of the Permian Jiamuhe Formation sandstones. During this period, laumontite was strongly dissolved, which significantly improved the reservoir porosity (Yuan et al., 2017). Thus, the average porosity of sandstone reservoirs increased to greater than 12%, with sandstones not exhibiting as the tight ones in this period. With subsequent tectonic subsidence, mechanical compaction continued to destroy the primary and laumontite dissolution pores, gradually decreasing the reservoir porosity. At the later stage of the diagenetic sequence, small amounts of calcite cementation marginally destroyed the reservoir quality with further porosity and permeability loss. According to analysis of the oil accumulation process, two stages of oil emplacement were identified in the Permian Jiamuhe Formation sandstone reservoir (Yuan et al., 2017). According to the average porosity evolution process, the first stage of oil emplacement occurred after laumontite dissolution, before the final consolidation of the sandstone reservoirs. The second stage of oil emplacement, however, generally took place following the tight sandstone formation time. Therefore, laumontite cementation and dissolution, the distribution of laumontite dissolution pores, and the fairways of the first stage of oil emplacement are key issues in oil exploration studies of this type of tight sandstone reservoir.

CONCLUSIONS

Reservoir diagenesis is significantly different in the lacustrine tight sandstone reservoirs from western to eastern China. Rock composition is one of the most important factors of reservoir diagenesis. The relatively strong compaction occurred mainly in sandstones with high ductile rock fragments. For the sandstones dominated by detrital quartz and feldspar, the siliceous cementation, calcite cementation, and feldspar dissolution, are the major types of diagenesis. Zeolite cementation and laumontite dissolution occurred mainly in the tight sandstones consisting of volcanic rock fragments.

An integration of porosity evolution and oil emplacement was established in tight sandstone reservoirs based on the diagenesis characteristics and diagenetic sequence. The paleoburial depth (or time) of the major diagenetic events and the relationship between thin section porosity and helium porosity were included in the investigation of the porosity quantitative evolution. Oil emplacement was regarded as a special diagenetic event within the paragenetic sequence of the diagenesis processes.

The integration of diagenesis, porosity evolution, and oil emplacement of three typical tight sandstone reservoirs showed that the tight reservoirs dominated by different diagenesis encountered different porosity loss processes, influencing the amount of oil emplacement. Thus, studies on the integration of diagenesis, porosity evolution, and oil emplacement in tight sandstone reservoirs can provide important guidance to reservoir potential evaluations.

REFERENCES CITED

Ajdukiewicz, J. M., and R. H. Lander, 2010, Sandstone reservoir quality prediction: The state of the art: AAPG Bulletin, v. 94, no. 8, p. 1083–1091, doi:10.1306/intro060110.

Al Khalifah, H., P. W. J. Glover, and P. Lorinczi, 2020, Permeability prediction and diagenesis in tight carbonates using machine learning techniques: Marine and Petroleum Geology, v. 112, 104096, 33 p. doi:10.1016/j.marpetgeo.2019.104096.

Anovitz, L., D. Cole, G. Rother, L. Allard, A. Jackson, and K. Littrell, 2013, Diagenetic changes in macro- to nanoscale porosity in the St. Peter Sandstone: An (ultra) small angle neutron scattering and backscattered electron imaging analysis: Geochimica et Cosmochimica Acta, v. 102, p. 280–305, doi:10.1016/j.gca.2012.07.035.

Beard, D., and P. Weyl, 1973, Influence of texture on porosity and permeability of unconsolidated sand: AAPG Bulletin, v. 57, no. 2, p. 349–369, doi:10.1306/819A4272-16C5-11D7-8645000102C1865D.

Bjørlykke, K., 2014, Relationships between depositional environments, burial history and rock properties. Some principal aspects of diagenetic process in sedimentary basins: Sedimentary Geology, v. 301, p. 1–14, doi:10.1016/j.sedgeo.2013.12.002.

Bjørlykke, K., and J. Jahren, 2012, Open or closed geochemical systems during diagenesis in sedimentary basins: Constraints on mass transfer during diagenesis and the prediction of porosity in sandstone and carbonate reservoirs: AAPG Bulletin, v. 96, no. 12, p. 2193–2214, doi:10.1306/04301211139.

Busch, B., I. Becker, B. Koehrer, D. Adelmann, and C. Hilgers, 2019, Porosity evolution of two Upper Carboniferous tight-gas-fluvial sandstone reservoirs: Impact of fractures

and total cement volumes on reservoir quality: Marine and Petroleum Geology, v. 100, p. 376–390, doi:10.1016/j.marpetgeo.2018.10.051.

Cama, J., J. Ganor, C. Ayora, and A. C. Lasaga, 2000, Smectite dissolution kinetics at 80°C and pH 8.8: Geochimica et Cosmochimica Acta, v. 64, no. 15, p. 2701–2717, doi:10.1016/S0016-7037(00)00378-1.

Camp, W. K., 2008, Basin-centered gas or subtle conventional traps? *in* S. P. Cumella, K. W. Shanley, and W. K. Camp, eds., Understanding, exploring, and developing tight-gas sands. 2005 Vail Hedberg Conference: AAPG Hedberg Series 3, p. 49–61, doi:10.1306/13131049H33323

Cao, Y., K. Xi, K. Liu, R. Zhu, G. Yuan, X. Zhang, and M. Song, 2018, Reservoir properties characterization and its genetic mechanism for tight sandstone oil and gas reservoir in lacustrine basin: The case of the fourth Member of Lower Cretaceous Quantou Formation in the south Songliao Basin [in Chinese with English abstract]: Acta Petrolei Sinica, v. 39, no. 3, p. 247–265, doi:10.7623/syxb201803001.

Chen, D., Y. Zhu, and Y. Xia, 2015, Origin mechanism of tightness from the He 8 section sandstone reservoir in Gaoqiao area of Ordos basin, China [in Chinese with English abstract]: Chenji Xuebao, v. 33, no. 6, p. 1217–1223.

Chen, H., X. Zhu, C. Chen, W. Yin, Q. Zhang, and R. Shi, 2017, Diagenesis and hydrocarbon emplacement in the Upper Triassic Yanchang Formation tight sandstones in the southern Ordos Basin, China: Australian Journal of Earth Sciences, v. 64, no. 7, p. 957–980, doi:10.1080/08120099.2017.1375983.

Dong, T., S. He, D. Wang, and Y. Hou, 2014, Hydrocarbon migration and accumulation in the Upper Cretaceous Qingshankou Formation, Changling Sag, southern Songliao Basin: Insights from integrated analyses of fluid inclusion, oil source correlation and basin modelling: Journal of Asian Earth Sciences, v. 90, p. 77–87, doi:10.1016/j.jseaes.2014.04.002.

Duan, Y., C. Wang, C. Zheng, B. Wu, and G. Zheng, 2008, Geochemical study of crude oils from the Xifeng oilfield of the Ordos Basin, China: Journal of Asian Earth Sciences, v. 31, no. 4–6, p. 341–356, doi:10.1016/j.jseaes.2007.05.003.

Dutton, P. S., and G. R. Loucks, 2010, Diagenetic controls on the evolution of porosity and permeability in lower Tertiary Wilcox sandstones from shallow to ultradeep (200–6700 m) burial, Gulf of Mexico Basin, U.S.A.: Marine and Petroleum Geology, v. 27, no. 1, p. 69–81, doi:10.1016/j.marpetgeo.2009.08.008.

Folk, R. L., 1974, Petrology of sedimentary rocks: Austin, Texas, Hemphill Publishing, 182 p.

Friedman, N., and J. R. O'Neil, 1977, Compilation of stable isotope fractionation: Factors of geochemical interest: Washington, DC, US Geological Survey Professional Paper 440-KK, 117 p.

Gier, S., H. R. Worden, D. W. Johns, and H. Kurzweil, 2008, Diagenesis and reservoir quality of Miocene sandstones in the Vienna Basin, Austria: Marine and Petroleum Geology, v. 25, no. 8, p. 681–695, doi:10.1016/j.marpetgeo.2008.06.001.

Gluyas, J., and C. Cade, 1999, Prediction of porosity in compacted sands: AAPG Memoir, v. 69, p. 19–27.

Gluyas, J., and M. Coleman, 1992, Material flux and porosity changes during sediment diagenesis: Nature, v. 356, no. 6364, p. 52–54, doi:10.1038/356052a0.

Gluyas, J., C. Garland, N. H. Oxtoby, and J. C. Hogg, 2000, Quartz cement: The Miller's tale, *in* R. H. Worden and S. Morad, eds., Quartz cementation in sandstones: New York, Wiley, p. 199–218, doi:10.1002/9781444304237.ch14.

Guo, S., X. Lyu, and Y. Zhang, 2018, Relationship between tight sandstone reservoir formation and hydrocarbon charging: A case study of a Jurassic reservoir in the eastern Kuqa Depression, Tarim Basin, NW China: Journal of Natural Gas Science and Engineering, v. 52, p. 304–316, doi:10.1016/j.jngse.2018.01.031.

Houseknecht, W. D., 1987, Assessing the relative importance of compaction processes and cementation to reduction of porosity in sandstones: AAPG Bulletin, v. 71, p. 633–642.

Hyodo, A., K. Kozdon, D. A. Pollington, and W. J. Valley, 2014, Evolution of quartz cementation and burial history of the Eau Claire Formation based on in situ oxygen isotope analysis of quartz overgrowths: Chemical Geology, v. 384, p. 168–180, doi:10.1016/j.chemgeo.2014.06.021.

Jia, C., M. Zheng, and Y. Zhang, 2012, Unconventional hydrocarbon resources in China and the prospect of exploration and development: Petroleum Exploration and Development, v. 39, no. 2, p. 139–146, doi:10.1016/S1876-3804(12)60026-3.

Kang, X., W. Hu, J. Cao, H. Wu, B. Xiang, and J. Wang, 2019, Controls on reservoir quality in fan-delta conglomerates: Insight from the lower Triassic Baikouquan Formation, Junggar Basin, China: Marine and Petroleum Geology, v. 103, p. 55–75, doi:10.1016/j.marpetgeo.2019.02.004.

Kolchugin, A., A. Immenhauser, B. Walter, and V. Morozov, 2016, Diagenesis of the palaeo-oil-water transition zone in a Lower Pennsylvanian carbonate reservoir: Constraints from cathodoluminescence microscopy, microthermometry, and isotope geochemistry: Marine and Petroleum Geology, v. 72, p. 45–61, doi:10.1016/j.marpetgeo.2016.01.014.

Lai J., G. Wang, J. Chen, S. Wang, Z. Zhou, and X. Fan, 2017, Origin and distribution of carbonate cement in tight sandstones: The Upper Triassic Yanchang Formation Chang 8 oil layer in West Ordos Basin, China: Geofluids, v. 2017, 8681753, 13 p., doi:10.1155/2017/8681753.

Lai, J., G. Wang, Y. Ran, Z. Zhou, and Y. Cui, 2016, Impact of diagenesis on the reservoir quality of tight oil sandstones: The case of Upper Triassic Yanchang Formation Chang 7 oil layers in Ordos Basin, China: Journal of Petroleum Science Engineering, v. 145, p. 54–65, doi:10.1016/j.petrol.2016.03.009.

Lai, J., G. Wang, S. Wang, J. Cao, M. Li, X. Pang, and Z. Zhou, 2018, Review of diagenetic facies in tight sandstones: Diagenesis, diagenetic minerals, and prediction via well logs: Earth-Science Reviews, v. 185, p. 234–258, doi:10.1016/j.earscirev.2018.06.009.

Lander, R. H., and L. M. Bonnell, 2010, A model for fibrous illite nucleation and growth in sandstones: AAPG Bulletin, v. 94, no. 8, p. 1161–1187, doi:10.1306/04211009121.

Li, D., C. Dong, C. Lin, L. Ren, T. Jiang, and Z. Tang, 2013, Control factors on tight sandstone reservoirs below source rocks in the Rangzijing slope zone of southern Songliao Basin, East China: Petroleum Exploration and Development, v. 40, no. 6, p. 742–750, doi:10.1016/S1876-3804(13)60099-3.

Li, X., X. Liu, S. Zhou, H. Liu, Q. Chen, J. Wang, J. Liao, and J. Huang, 2012, Hydrocarbon origin and reservoir forming model of the Lower Yanchang Formation, Ordos Basin: Petroleum Exploration and Development, v. 39, no. 2, p. 184–193, doi:10.1016/S1876-3804(12)60031-7.

Li, Y., X. Chang, W. Yin, T. Sun, and T. Song, 2017, Quantitative impact of diagenesis on reservoir quality of the Triassic Chang 6 tight oil sandstones, Zhenjing area, Ordos Basin, China: Marine and Petroleum Geology, v. 86, p. 1014–1028, doi:10.1016/j.marpetgeo.2017.07.005.

Lothe, A., B. Emmel, P. Bergmo, I. Akervoll, J. Todorovic, M. Bhuiyan, and J. Knies, 2018, Porosity, permeability and compaction trends for Scandinavian regoliths: Marine and Petroleum Geology, v. 92, p. 319–331, doi:10.1016/j.marpetgeo.2017.10.027.

Lundegard, P., 1992, Sandstone porosity loss - A "big picture" view of the importance of compaction: Journal of Sedimentary Petrology, v. 62, no. 2, p. 250–260, doi:10.1306/D42678D4-2B26-11D7-8648000102C1865D.

Ma, P., C. Lin, S. Zhang, C. Dong, Y. Zhao, D. Dong, K. Shehzad, A. Muhammad, D. Guo, and X. Mu, 2018, Diagenetic history and reservoir quality of tight sandstones: A case study from Shiqianfeng sandstones in upper Permian of Dongpu Depression, Bohai Bay Basin, eastern China: Marine and Petroleum Geology, v. 89, no. 2, p. 280–299, doi:10.1016/j.marpetgeo.2017.09.029.

Mahmic, O., H. Dypvik, and E. Hammer, 2018, Diagenetic influence on reservoir quality evolution, examples from Triassic conglomerates/arenites in the Edvard Grieg field, Norwegian North Sea: Marine and Petroleum Geology, v. 93, p. 247–271, doi:10.1016/j.marpetgeo.2018.03.006.

Marcussen, Ø., T. E. Maast, N. H. Mondol, J. Jahren, and K. Bjørlykke, 2010, Changes in physical properties of a reservoir sandstone as a function of burial depth – The Etive Formation, northern North Sea: Marine and Petroleum Geology, v. 27, no. 8, p. 1725–1735, doi:10.1016/j.marpetgeo.2009.11.007.

Metwally, M. Y., and M. E. Chesnokov, 2012, Clay mineral transformation as a major source for authigenic quartz in thermo-mature gas shale: Applied Clay Science, v. 55, p. 138–150, doi:10.1016/j.clay.2011.11.007.

Mohammed Sajed, O. K., P. W. J. Glover, and R. E. L. Collier, 2021, Reservoir quality estimation using a new ternary diagram approach applied to carbonate formations in north-western Iraq: Journal of Petroleum Science Engineering, v. 196, 108024, 21 p., doi:10.1016/j.petrol.2020.108024.

Mondol, N. H., K. Bjørlykke, J. Jahren, and K. Høeg, 2007, Experimental mechanical compaction of clay mineral aggregates—Changes in physical properties of mudstones during burial: Marine and Petroleum Geology, v. 24, no. 5, p. 289–311, doi:10.1016/j.marpetgeo.2007.03.006.

Morad, S., K. Al-Ramadan, J. M. Ketzer, and L. F. DeRos, 2010, The impact of diagenesis on the heterogeneity of sandstone reservoirs: A review of the role of depositional facies and depositional facies and sequence stratigraphy: AAPG Bulletin, v. 94, no. 8, p. 1267–1309, doi:10.1306/04211009178.

Mu, N., Y. Fu, H. M. Schulz, and W. Berk, 2016, Authigenic albite formation due to water–rock interactions-case study: Magnus oilfield (UK, Northern North Sea): Sedimentary Geology, v. 331, p. 30–41, doi:10.1016/j.sedgeo.2015.11.002.

Oluwadebi, A., K. Taylor, and P. Dowey, 2018, Diagenetic controls on the reservoir quality of the tight gas Collyhurst Sandstone Formation, Lower Permian, East Irish Sea Basin, United Kingdom: Sedimentary Geology, v. 371, p. 55–74, doi:10.1016/j.sedgeo.2018.04.006.

Proia, A. D., and N. T. Brinn, 1985, Identification of calcium oxalate crystals using alizarin red S stain: Archives of Pathology & Laboratory Medicine, v. 109, no. 2, p. 186–189.

Rahman, M., and R. Worden, 2016, Diagenesis and its impact on the reservoir quality of Miocene sandstones (Surma Group) from the Bengal Basin, Bangladesh: Marine and Petroleum Geology, v. 77, p. 898–915, doi:10.1016/j.marpetgeo.2016.07.027.

Rashid, F., D. Hussein, P. W. J. Glover, P. Lorinczi, and J. A. Lawrence, 2022, Quantitative diagenesis: Methods for studying the evolution of the physical properties of tight carbonate reservoir rocks: Marine and Petroleum Geology, v. 139, 105603, 18 p., doi:10.1016/j.marpetgeo.2022.105603.

Robinson, A., and J. Gluyas, 1992, Duration of quartz cementation in sandstones, North Sea and Haltenbanken Basins: Marine and Petroleum Geology, v. 9, no. 3, p. 324–327, doi:10.1016/0264-8172(92)90081-O.

Rosales, I., L. Pomar, and S. Al-Awwad, 2018, Microfacies, diagenesis and oil emplacement of the Upper Jurassic Arab-D carbonate reservoir in an oil field in central Saudi Arabia (Khurais Complex): Marine and Petroleum Geology, v. 96, p. 551–576, doi:10.1016/j.marpetgeo.2018.05.010.

Sample, J. C., M. E. Torres, A. Fisher, W. Hong, C. Destrigneville, W. F. Defliese, and A. E. Tripati, 2017, Geochemical constraints on the temperature and timing of carbonate formation and lithification in the Nankai Trough, NanTroSEIZE transect: Geochimica et Cosmochimica Acta, v. 198, p. 92–114, doi:10.1016/j.gca.2016.10.013.

Schmoker, J. W., 2005, U.S. Geological Survey assessment concepts for continuous petroleum accumulations, *in* USGS Southwestern Wyoming Province Assessment Team, eds., Petroleum systems and geologic assessment

of oil and gas in the southwestern Wyoming province, Wyoming, Colorado, and Utah: Washington, DC, US Geological Survey Digital Data Series DDS-69-D, p. 1–7.

Stroker, M. T., B. N. Harris, C. W. Elliott, and M. J. Wampler, 2013, Diagenesis of a tight gas sand reservoir: Upper Cretaceous Mesaverde Group, Piceance Basin, Colorado: Marine and Petroleum Geology, v. 40, p. 48–68, doi:10.1016/j.marpetgeo.2012.08.003.

Taylor, T. R., M. R. Giles, L. A. Hathon, T. N. Diggs, N. R. Braunsdorf, G. V. Birbiglia, M. K. Kittridge, C. I. Macaulay, and I. S. Espejo, 2010, Sandstone diagenesis and reservoir quality prediction: Models, myths, and reality: AAPG Bulletin, v. 94, no. 8, p. 1093–1132, doi:10.1306/04211009123.

Tobin, R. C., T. McClain, R. B. Lieber, A. Ozkan, L. A. Banfield, A. M. Marchand, and L. E. McRae, 2010, Reservoir quality modeling of tight-gas sands in Wamsutter field: Integration of diagenesis, petroleum systems, and production data: AAPG Bulletin, v. 94, no. 8, p. 1229–1266, doi:10.1306/04211009140.

Walker, E., and P. W. J. Glover, 2018, Measurements of the relationship between microstructure, pH, and the streaming and zeta potentials of sandstones: Transport in Porous Media, v. 121, no. 1, p. 183–206, doi:10.1007/s11242-017-0954-5.

Wang, G., X. Chang, W. Yin, Y. Li, and T. Song, 2017, Impact of diagenesis on reservoir quality and heterogeneity of the Upper Triassic Chang 8 tight oil sandstones in the Zhenjing area, Ordos Basin, China: Marine and Petroleum Geology, v. 83, p. 84–96, doi:10.1016/j.marpetgeo.2017.03.008.

Wang, W., and Q. Yue, 2012, Genetic mechanisms for tight sandstone reservoir of Xujiahe formation, north Sichuan Basin [in Chinese with English abstract]: Natural Gas Exploration and Development, v. 35, p. 13–17.

Wang, Y., Y. Cao, K. Xi, G. Song, and H. Liu, 2013, A recovery method for porosity evolution of clastic reservoirs with geological time: A case study of the Es4s submember in the Dongying Depression, Jiyang Subbasin [in Chinese with English abstract]: Acta Petrolei Sinica, v. 34, no. 6, p. 1100–1111, doi:10.7623/syxb201306008.

Wang, Y., M. Lin, K. Xi, Y. Cao, J. Wang, G. Yuan, K. Muhammad, and M. Song, 2018, Characteristics and origin of the major authigenic minerals and their impacts on reservoir quality in the Permian Wutonggou Formation of Fukang Sag, Junggar Basin, western China: Marine and Petroleum Geology, v. 97, p. 241–259, doi:10.1016/j.marpetgeo.2018.07.008.

Wei, W., X. Zhu, Y. Meng, L. Xiao, M. Xue, and J. Wang, 2016, Porosity model and its application in tight gas sandstone reservoir in the southern part of West Depression, Liaohe Basin, China: Journal of Petroleum Science Engineering, v. 141, p. 24–37, doi:10.1016/j.petrol.2016.01.010.

Wilson, L., M. Wilson, J. Green, and I. Patey, 2014, The influence of clay mineralogy on formation damage in North Sea reservoir sandstones: A review with illustrative examples: Earth-Science Reviews, v. 134, p. 70–80, doi:10.1016/j.earscirev.2014.03.005.

Worden, R. H., and S. D. Burley, 2003, Sandstone diagenesis: The evolution of sand to stone, *in* S. D. Burley and R. H. Worden, eds., Sandstone diagenesis: Recent and ancient: New York, Wiley, p. 1–44, doi:10.1002/9781444304459.ch.

Wu, L., C. Zhou, J. Keeling, D. Tong, and W. Yu, 2012, Towards an understanding of the role of clay minerals in crude oil formation, migration and accumulation: Earth-Science Reviews, v. 115, no. 4, p. 373–386, doi:10.1016/j.earscirev.2012.10.001.

Xi, K., Y. Cao, J. Jahren, R. Zhu, K. Bjørlykke, B. Haile, L. Zheng, and H. Hellevang, 2015a, Diagenesis and reservoir quality of the Lower Cretaceous Quantou Formation tight sandstones in the southern Songliao Basin, China: Sedimentary Geology, v. 330, p. 90–107, doi:10.1016/j.sedgeo.2015.10.007.

Xi, K., Y. Cao, M. Lin, K. Liu, S. Wu, G. Yuan, and T. Yang, 2019a, Applications of light stable isotopes (C, O, H) in the study of sandstone diagenesis: A review: Acta Geologica Sinica, v. 93, no. 1, p. 213–226, doi:10.1111/1755-6724.13769.

Xi, K., Y. Cao, K. Liu, J. Jahren, R. Zhu, G. Yuan, and H. Hellevang, 2019b, Authigenic minerals related to wettability and their impacts on oil accumulation in tight sandstone reservoirs: An example from the Lower Cretaceous Quantou Formation in the southern Songliao Basin, China: Journal of Asian Earth Sciences, v. 178, p. 173–192, doi:10.1016/j.jseaes.2018.04.025.

Xi, K., Y. Cao, K. Liu, S. Wu, G. Yuan, R. Zhu, K. Muhammad, and Y. Zhao, 2019c, Diagenesis of tight sandstone reservoirs in the Upper Triassic Yanchang Formation, southwestern Ordos Basin, China: Marine and Petroleum Geology, v. 99, p. 548–562, doi:10.1016/j.marpetgeo.2018.10.031.

Xi, K., Y. Cao, K. Liu, S. Wu, G. Yuan, R. Zhu, Y. Zhao, and H. Hellevang, 2019d, Geochemical constraints on the origins of calcite cements and their impacts on reservoir heterogeneities: A case study on tight oil sandstones of the Upper Triassic Yanchang Formation, Southwestern Ordos Basin, China: AAPG Bulletin, v. 103, no. 10, p. 2447–2485, doi:10.1306/01301918093.

Xi, K., Y. Cao, Y. Wang, Q. Zhang, J. Jin, R. Zhu, S. Zhang, J. Wang, T. Yang, and L. Du, 2015b, Factors influencing physical property evolution in sandstone mechanical compaction: The evidence from diagenetic simulation experiments: Petroleum Science, v. 12, no. 3, p. 391–405, doi:10.1007/s12182-015-0045-6.

Yang, T., Y. Cao, Y. Wang, H. Friis, B. Haile, K. Xi, and H. Zhang, 2016, The coupling of dynamics and permeability in the hydrocarbon accumulation period controls the oil-bearing potential of low permeability reservoirs: A case study of the low permeability turbidite reservoirs in the middle part of the third member of Shahejie Formation in Dongying Sag: Petroleum Science, v. 13, no. 2, p. 204–224, doi:10.1007/s12182-016-0099-0.

Yuan, G., Y. Cao, L. Qiu, and Z. Chen, 2017, Genetic mechanism of high-quality reservoirs in Permian tight fan delta conglomerates at the northwestern margin of the Junggar

basin, northwestern China: AAPG Bulletin, v. 101, no. 12, p. 1995–2019, doi:10.1306/02071715214.

Zhang, L., Y. Soong, R. Dilmore, and C. Lopano, 2015, Numerical simulation of porosity and permeability evolution of Mount Simon sandstone under geological carbon sequestration conditions: Chemical Geology, v. 403, p. 1–12, doi:10.1016/j.chemgeo.2015.03.014.

Zhang, S., 2008, Tight sandstone gas reservoirs: Their origin and discussion [in Chinese with English abstract]: Oil and Gas Geology, v. 29, p. 1–10, doi:10.11743/ogg20080101.

Zhang, W., Y. Li, T. Xu, H. Cheng, Y. Zheng, and P. Xiong, 2009, Long-term variations of CO_2 trapped in different mechanisms in deep saline formations: A case study of the Songliao Basin, China: International Journal of Greenhouse Gas Control, v. 3, no. 2, p. 161–180, doi:10.1016/j.ijggc.2008.07.007.

Zhao, J., N. P. Mountney, C. Liu, H. Qu, and J. Lin, 2015, Outcrop architecture of a fluviolacustrine succession: Upper Triassic Yanchang Formation, Ordos Basin China: Marine and Petroleum Geology, v. 68, no. A, p. 394–413, doi:10.1016/j.marpetgeo.2015.09.001.

Zhao, W., D. Dong, J. Li, and G. Zhang, 2012, The resource potential and future status in natural gas development of shale gas in China: Engineering and Science, v. 14, no. 7, p. 46–52.

Zhou, Y., Y. Ji, L. Xu, S. Che, X. Niu, L. Wan, Y. Zhou, Z. Li, and Y. You, 2016, Controls on reservoir heterogeneity of tight sand oil reservoirs in Upper Triassic Yanchang Formation in Longdong Area, southwest Ordos Basin, China: Implications for reservoir quality prediction and oil accumulation: Marine and Petroleum Geology, v. 78, p. 110–135, doi:10.1016/j.marpetgeo.2016.09.006.

Zou, C., Z. Yang, S. Tao, X. Yuan, R. Zhu, L. Hou, S. Wu, et al., 2013a, Continuous hydrocarbon accumulation over a large area as a distinguishing characteristic of unconventional petroleum: The Ordos Basin, North-Central China: Earth-Science Reviews, v. 126, p. 358–369, doi:10.1016/j.earscirev.2013.08.006.

Zou, C., Z. Yang, G. Zhang, L. Hou, R. Zhu, and S. Tao, 2014, Conventional and unconventional petroleum "orderly accumulation": Concept and practical significance: Petroleum Exploration and Development, v. 41, no. 1, p. 14–30, doi:10.1016/S1876-3804(14)60002-1.

Zou, C., G. Zhang, Z. Yang, S. Tao, L. Hou, and R. Zhu, 2013b, Concepts, characteristics, potential and technology of unconventional hydrocarbons: On unconventional petroleum geology: Petroleum Exploration and Development, v. 40, no. 4, p. 413–428, doi:10.1016/S1876-3804(13)60053-1.

Zou, C., R. Zhu, K. Liu, L. Su, B. Bai, and X. Zhang, 2012, Tight gas sandstone reservoirs in China: Characteristics and recognition criteria: Journal of Petroleum Science Engineering, v. 88–89, p. 82–91, doi:10.1016/j.petrol.2012.02.001.